0 0 0 4 3 0 3 4 2 9

LBL-3798

RECEIVED
LAWRENCE
BERKELEY LABORATORY

OCT 30 1975

LIBRARY AND
DOCUMENTS SECTION

VIBRATIONAL INELASTICITY IN H_2 COLLISIONS WITH He AND Li^+

Andrew Wesley Raczkowski
(Ph. D. thesis)

September 1975

Prepared for the U. S. Energy Research and
Development Administration under Contract W-7405-ENG-48

For Reference

Not to be taken from this room

LAWRENCE BERKELEY LABORATORY
UNIVERSITY OF CALIFORNIA
BERKELEY

LBL-3798

DISCLAIMER

This document was prepared as an account of work sponsored by the United States Government. While this document is believed to contain correct information, neither the United States Government nor any agency thereof, nor the Regents of the University of California, nor any of their employees, makes any warranty, express or implied, or assumes any legal responsibility for the accuracy, completeness, or usefulness of any information, apparatus, product, or process disclosed, or represents that its use would not infringe privately owned rights. Reference herein to any specific commercial product, process, or service by its trade name, trademark, manufacturer, or otherwise, does not necessarily constitute or imply its endorsement, recommendation, or favoring by the United States Government or any agency thereof, or the Regents of the University of California. The views and opinions of authors expressed herein do not necessarily state or reflect those of the United States Government or any agency thereof or the Regents of the University of California.

0 0 0 0 4 3 0 3 4 3 0

Contents

Abstract v

I. Introduction. 1

II. Theory 4

A. The N-Coupled Channel Problem. 4

B. Classical S-Matrix Theory and Partial Averaging. 25

C. Rate Constants and Relaxation Times. 39

III. Calculations and Results. 48

A. H_2-Li^+ 54

B. H_2-He 89

IV. Conclusions 118

Acknowedgments 122

References. 123

0 0 0 0 4 3 0 3 4 3 1

VIBRATIONAL INELASTICITY IN H_2 COLLISIONS WITH He AND Li^+

Andrew Wesley Raczkowski

Inorganic Materials Research Division, Lawrence Berkeley Laboratory
and Department of Chemistry; University of California,
Berkeley, California 94720

Abstract

The partially averaged version of classical S-matrix theory was applied to three-dimensional collisions of H_2 with He and Li^+. For H_2-Li^+, cross-sections for the de-excitation of H_2 from $(n_1,j_1) = (1,0)$ to the ground vibrational manifold were computed at a total energy of 1.2 eV and compared to previously done coupled channel calculations of Schaefer and Lester. The agreement is very good. For H_2-He, the Kutzelnigg-Tsapline interaction potential was extended to small atom-diatom separations, the ab initio points were then fit to an analytic form, and cross-sections for the de-excitation of H_2 from the states (n_1,j_1), $n_1 = 1$, $j_1 = 0,2,4$ to the ground vibrational manifold were computed at total energies of .9, 1.1, 1.3 and 1.5 eV. For comparison, coupled channel calculations were also performed on the system at the same energies. The agreement was poorer than in the H_2-Li^+ case, for identifiable reasons. The cross-sections were used to compute rate constants and relaxation times for the H_2-He system. Comparison of these results with the results of experiment and of other calculations shows good agreement, certainly within the expected errors.

I. INTRODUCTION

In essence, the present work describes several calculations performed by the author under the tutelage of Professor William H. Miller. These computational studies were a continuation of efforts to develop a reliable method of performing non-reactive scattering calculations, based on the Miller formulation of multi-dimensional classical-limit quantum mechanics. The theory was first applied to vibrationally inelastic collinear collisions and the rigid-rotor problem (Miller, 1970, 1971) to calculate specific S-matrix elements. The development of complex-valued trajectories (Miller and George, 1972) allowed the extension of the theory to classically forbidden transitions, resulting in calculation of S-matrix elements for vibrationally inelastic three-dimensional atom-diatom collisions (Doll and Miller, 1972).

The scope of the present work is the description of the next step in this sequence, namely, the incorporation of the partial-averaging procedure, a labor-saving device which allows direct calculation of cross-sections without recourse to S-matrix elements as intermediates (Miller and Raczkowski, 1972). The two sets of calculations described were done on H_2-Li^+ and H_2-He, respectively. The choice of H_2 plus a monatomic collision partner was not made because of intrinsic interest in H_2. Rather, the choice was determined by the following arguments. First, because of the light masses of the atoms involved, these systems should manifest the most pronounced quantum effects and thus serve as an acid test of any classical-limit method. Secondly, because of the small number of electrons in the system, reliable <u>ab initio</u> interaction-potential surfaces exist for both

systems, thus obviating any difficulties about choice of potential surface. One might add parenthetically that the internal potential of H_2 is firmly established by the work of Kolos and Wolniewicz. Thirdly, because of the wide spacing of the H_2 energy levels, reliable coupled-channel calculations were feasible for both systems, providing a standard of comparison for the classical-limit results. And lastly, the work of Audibert, Joffrin and Ducuing has raised the possibility of comparison, albert indirect, of computations with experiment.

Before beginning the discussion of computational techniques and results it seems appropriate to give a description of the theory behind the computation. Chapter II provides this description, which is meant to serve three purposes. First, it should give the reader some appreciation for the similarities and differences between the two scattering methods being considered, i.e., coupled-channel and classical-limit. Secondly, it should serve to define notation. Lastly, it should give an idea of the amount of averaging over cross-sections required to obtain the quantity comparable to experiment, i.e, how indirect is the comparison alluded to above.

Chapter III gives a detailed account of the calculations performed. It begins with a specific statement of the problems involved in applying the classical-limit approach and then goes on to present the computational techniques used to overcome the difficulties. The relative success or failure of each technique is indicated, and where possible, the reasons for failure are stated. The emphasis of the chapter is on techniques rather than results, because the results

for H_2-Li^+ have already been discussed in the literature (Raczkowski and Miller, 1974), and the H_2-He system will be the subject of forthcoming journal articles. The literature contains only a hazy outline of the methods used to apply the classical-limit formalism, thus it seems more appropriate to present a thorough discussion of techniques. However, the study of techniques is applied mathematics; science is the study of nature. When one has done careful calculations on a real system it is difficult to repress one's desire to discuss the results, and thus a short discussion was included for both systems.

II. THEORY

The theoretical basis of the calculations described in this work, i.e., the N-coupled channel problem, classical-limit quantum mechanics, and the relationship of cross sections to rate constants and relaxation times, are all well discussed in the literature. The present discussion, therefore, will be restricted to a summary of those aspects most germane to the calculations described in the next chapter. Its inclusion is meant to serve three purposes: (1) completeness, (2) providing a conceptual background for the uninitiated reader, and (3) establishing the notation to be used in subsequent chapters. In particular, the present discussion will avoid all proofs. Results will be stated, and at appropriate points in the discussion, the interested reader will be referred to the sources in the literature which most closely parallel the discussion here.

A. The N-Coupled Channel Problem

This section gives a discussion of quantum scattering theory, as it applies to the problem of interest. The kinematics are discussed first, the scattering problem is then formulated in terms of the S-matrix. The S-matrix contains all possible scattering information. Its knowledge is equivalent to knowledge of the solution to the full Schroedinger Equation for the problem. The section concludes with a description of the coupled channel approach to the solution of the Schroedinger Equation and assembling of the S-matrix, and an outline of the numerical method of Gordon (Gordon, 1969, 1971), chosen to obtain the solution.

The specific problem under discussion is a non-reactive atom-diatom

collision. (The two cases presented in the next chapter are $H_2 + Li^+$, and H_2 + He. In the first of these, the "atom" is actually an ion. However, its charge enters the problem only in terms of the specific form of the potential. The general description of the collision process is unaffected.) Let A designate the atom and B-C the diatomic. Eliminating center-of-mass motion, one can describe the system (Fig. 1) by defining $\vec{r}$ as the distance from B to C, and $\vec{R}$ as the distance from the B-C center-of-mass to A. Let m be the reduced mass of B-C, μ be the reduced mass of A and the diatomic, $\vec{p}$ and $\vec{P}$ be the momentum operators corresponding to $\vec{r}$ and $\vec{R}$, resp., and for future use, define γ as:

$$\gamma = \text{Arccos}\ (\hat{R} \cdot \hat{r}). \tag{2.1}$$

(as usual, $R = |\vec{R}|$, and $\hat{R} = \vec{R}/R$, and similarly for $\vec{r}$). γ, then, is the angle between the vectors $\vec{r}$, and $\vec{R}$. With these definitions, the Hamiltonian for the system may be written:

$$H = \frac{P^2}{2\mu} + \frac{p^2}{2m} + V_T\ (\vec{r}, \vec{R}), \tag{2.2}$$

where V_T is the total potential energy of the system. One notes that if the atom is assumed structureless, and if the diatomic is in a Σ electronic state, V_T depends only on the magnitudes of $\vec{r}$ and $\vec{R}$, and on the angle between them. (Lester, 1973)

$$V_T\ (\vec{r}, \vec{R}) = V_T\ (r, R, \gamma) \tag{2.3}$$

Further, let v(r) represent the potential of the free B-C diatomic, in the absence of A. One can then define an interaction potential, V_I, by

$$V_I\ (r, R, \gamma) = V_T\ (r, R, \gamma) - v(r). \tag{2.4}$$

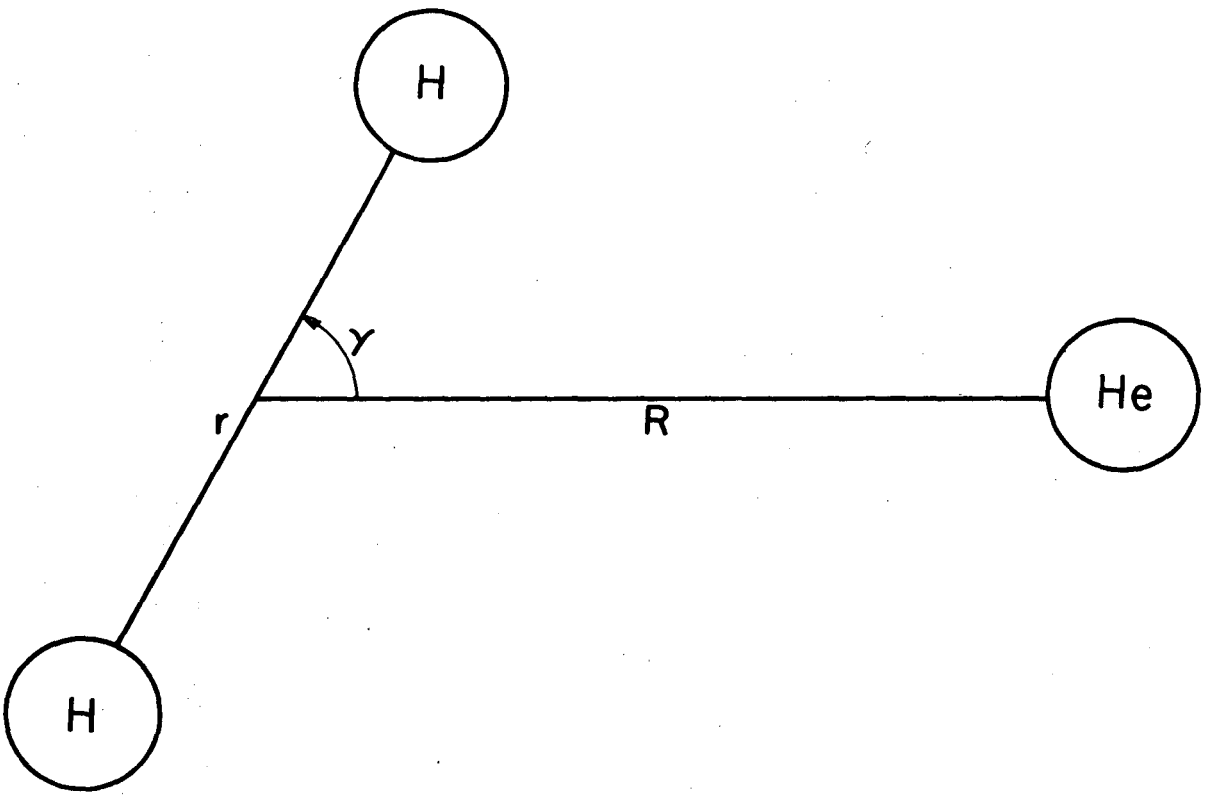

XBL 759-7221

Fig. 1. Coordinates for H_2-He system.

This is possible because the energy range of the calculations was chosen so as to exclude any bound states of A-C or A-B, or dissociation of B-C, thus the diatomic maintains its identity throughout the collision, and Eq. (2.4) defines a unique interaction potential. The Hamiltonian then becomes

$$H = \frac{P^2}{2\mu} + \frac{p^2}{2m} + v(r) + V_I(r, R, \gamma) \tag{2.5a}$$

$$= H_o + V_I(r, R, \gamma) \tag{2.5b}$$

where the definition of H_o is obvious. Now, in both systems of interest, the interaction potential falls off sufficiently fast with increasing R that one can define an asymptotic region ($R \to \infty$), where $H \to H_o$. The allowed scattering states asymptotically satisfy

$$H_o \phi(\vec{r}, \vec{R}) = E \cdot \phi(\vec{r}, \vec{R}) \tag{2.6}$$

where E is the energy of an asymptotic state ϕ. For definiteness, one may consider the scattering of some wave-packet $\psi(t)$ in the Schroedinger picture. Set $\psi = \psi(0)$, then $\psi(t)$ is given by the action of the propagator on $\psi(0)$; (Taylor, 1972)

$$\psi(t) = \exp\left(\frac{iHt}{\hbar}\right) \cdot \psi(0) \tag{2.7a}$$

then the incoming and outgoing asymptotic states are given by the relations:

$$\lim_{t \to -\infty} \exp\left(\frac{-iHt}{\hbar}\right) \cdot \psi = \lim_{t \to -\infty} \exp\left(\frac{-iH_o t}{\hbar}\right) \cdot \phi in \tag{2.7b}$$

$$\lim_{t \to +\infty} \exp\left(\frac{-iHt}{\hbar}\right) \cdot \psi = \lim_{t \to +\infty} \exp\left(\frac{-iH_o t}{\hbar}\right) \cdot \phi out \tag{2.7c}$$

Not surprisingly, the eigenstates of H_o will play an important role in the development of this section, since the asymptotes are most naturally expressed in terms of these functions. Fortunately, these

functions are easily found. (Lester, 1975). One first notes that H_o is separable in the sense that there are no terms simultaneously involving $\vec{r}$ and $\vec{R}$. One then proceeds in the time-honored tradition, letting

$$\phi(\vec{r}, \vec{R}) = X(\vec{r}) \cdot U(\vec{R}) \tag{2.8}$$

and substituting into Eq. (2.6), one obtains the system of equations:

$$\left(\frac{P^2}{2\mu} - E_{tr}\right) U(\vec{R}) = 0 \tag{2.9a}$$

$$\left(\frac{p^2}{2m} + v(r) - E_{int}\right) X(\vec{r}) = 0 \tag{2.9b}$$

$$E_{tr} + E_{int} = E \tag{2.9c}$$

For the moment, E_{tr} and E_{int} should be viewed as some partitioning of the total energy E such that Eqs. (2.9) are satisfied. Later, of course, they will be shown to be the translational and internal energies, respectively. One next transforms to polar co-ordinates, and letting P_R, (p_r) and $\ell(j)$ be the radial and angular momentum operators for the relative (internal) motion, one obtains:

$$\left(\frac{P_R^2}{2\mu} + \frac{\ell^2}{2\mu R^2} - E_{tr}\right) U(\vec{R}) = 0 \tag{2.10a}$$

$$\left(\frac{P_r^2}{2m} + \frac{j^2}{2mR^2} - E_{int}\right) X(\vec{r}) = 0 \tag{2.10b}$$

Finally, substitution of:

$$U(\vec{R}) = \frac{1}{R} u_{k\ell}(R)\, Y^{\ell}_{m_\ell}(\hat{R}) \tag{2.11a}$$

$$X(\vec{r}) = \frac{1}{r} \chi_{nj}(r)\, Y^{j}_{m_j}(\hat{r}) \tag{2.11b}$$

into Eqs. (2.10) yields the familiar free particle solutions for $u_{k\ell}(R)$:

$$u_{k\ell}(R) = a \cdot (kR)\, j_\ell(kR) + b \cdot (kR)\, n_\ell(kR) \tag{2.12a}$$

where a and b are expansion coefficients, $j_\ell(n_\ell)$ is the regular (irregular) spherical Bessel function of order ℓ, and k is the usual wave vector; defined in terms of the translational energy as:

$$k = \frac{1}{\hbar}(2\mu E_{tr})^{1/2} \tag{2.12b}$$

Equation (2.10b) reduces to a one-dimensional eigenvalue problem;

$$\left(\frac{p^2}{2m} + \frac{\hbar^2 j(j+1)}{2mr^2} + v(r) - \varepsilon_{nj}\right) \chi_{nj}(r) = 0 \tag{2.12c}$$

where p is just a one-dimensional momentum operator. Equation (2.12c) is just the defining equation for the bound vibration-rotation states χ_{nj} of the B-C diatomic which correspond to internal excitation energy ε_{nj}. Because the energy range studied is below the dissociation energy of the diatomic, it is legitimate to restrict the solutions of Eq. (2.12c) and its antecedents to bound states. One might add, as a procedural point, that ε_{oo} will be defined as being zero, thus fixing the energy scale. With this definition, states of total energy E will be scattering states with at least one particle asymptotically free if E>0, and three-particle bound states if E>0.

At this point, the kinematics and notation have been established, and the next topic to be discussed is the S-matrix. With Eqs. (2.7b, c) as motivation, it is convenient to define the two Moller operators (Taylor, 1972). Let U (U_o) represent the propagator corresponding to H (H_o), then:

$$\Omega_+ = \lim_{t\to-\infty} U(t)^\dagger U_o(t) = \lim_{t\to-\infty} e^{\frac{-iHt}{\hbar}} e^{\frac{-iH_o t}{\hbar}}, \tag{2.13a}$$

$$\Omega_- = \lim_{t\to+\infty} U(t)^\dagger U_o(t) = \lim_{t\to+\infty} e^{\frac{-iHt}{\hbar}} e^{\frac{-iH_o t}{\hbar}} \tag{2.13b}$$

In analogy with Eqs. (2.7b, c) one has the relations:

$$\psi = \Omega_+ \cdot \phi_{in}, \tag{2.14a}$$

$$\psi = \Omega_- \cdot \phi_{out}, \tag{2.14b}$$

which relate the actual scattering state to its two asymptotes. One then has:

$$\phi_{out} = \Omega_-^\dagger \psi = \Omega_-^\dagger \Omega_+ \phi_{in} \tag{2.15}$$

where one has substitutal Eq. (2.14b) for ψ. If one then defines the product of Moller operators in Eq. (2.15) as being the S- or scattering operator, one can write:

$$\phi_{out} = S \phi_{in} \tag{2.16}$$

It is clear that by acting on the incoming states, the S-operator directly yields the outgoing state. Its action is exactly equivalent to solution of the full Schroedinger Equation (SE) with the same incoming boundary condition and passage to the asymptotic limit for the outgoing component of the solution. At first one might think that solution of the full S.E. yields more information, since one also gets the solution for small interparticle separations. However, this information is of no particular interest. Operationally, one may define the asymptotic region as one where the interaction potential is small with respect to the relative translational energy. In the calculations described in the next chapter, the translational energies were on the order of 0.5 eV; the interaction potentials were less than 0.5°K, (one part in 10^4 of the translational energy) for atom-diatom separations of ten or so Angstroms, (about 10^{-7} cm). Thus if one considers a scattering experiment taking place in an apparatus of human dimensions, i.e., detector separated from scattering

established in Eqs. (2.12). Further, if one seriously believes the statement about the equivalence of the S-operator to the solution of the full S.E. and passage to the asymptotic limit, one must conclude that the S-operator's conservation properties reflect those of the full Hamiltonian. In particular, (Taylor, 1972) one can establish that they both conserve total energy and angular momentum. By contrast, the asymptotic Hamiltonian separately conserves energy and angular momentum for both the translational and internal motions. The effect of the interaction potential, then, is to conserve total energy and angular momentum, but possibly reapportion that total between the translational and internal modes. In employing the coupled channel formalism, one wishes to make maximum use of these conservation properties. As was seen earlier, the wavefunctions are described asymptotically as a superposition of terms like:

$$\phi(\vec{r}, \vec{R}; E, n, j, m_j, \ell, m_\ell) = \frac{1}{rR} u_{k\ell}(\vec{R}) \chi_{nj}(\vec{r}) Y^{\ell}_{m_\ell}(\hat{R}) \times Y^{j}_{m_j}(\hat{r}) \tag{2.19}$$

Because of total angular-momentum conservation, it is convenient to transform from the uncoupled basis (ℓ, m_ℓ, j, m_j) to the coupled basis (J, M, j, ℓ), where as usually J is the total angular momentum and M is its projection along some space-fixed axis. (Since the total system is rotationally invariant, the choice of the M defining axis is not critical. More will be said about this later.) The transformation is effected by the usual coupling relations involving Clebsch-Gordon Coefficients: (Rose, 1957)

event by distances on the scale of centimeters, there is no doubt that only the asymptotic form of the wavefunction is being probed. Not suprisingly then, the usual quantities of interest in a scattering experiment, such as cross sections, phase shifts, etc. all depend on the asymptotic form of the wavefunction. Thus all such scattering information is obtainable from the S-operator.

Returning then, to the main thread of the discussion, if one knows the incoming state of the system, say ϕ_1, it is reasonable to ask what is the likelihood of emerging in various possible final states of the system, say ϕ_2. Now, from Eq. (2.16):

$$\phi_{out} = S \cdot \phi_1 \tag{2.17}$$

and the probability of emerging in state ϕ_2 is

$$P_{1\to 2} = |(\phi_2|\phi_{out})|^2 = |(\phi_2|S|\phi_1)|^2 \tag{2.18}$$

Equation (2.18) leads immediately to the concept of an S-matrix. If one chooses a suitable basis set for the asymptotic region, one could evaluate the integrals of the S-operator between each pair of basis functions (thus defining the S-matrix; eg, the integral appearing in Eq. (2.18) would be the element S_{12}) and store the results. In the usual matrix-mechanics way, one would then express any integral of the S-operator by expanding the in and out states in terms of the chosen basis set.

The choice of an appropriate basis set representation is, not suprisingly, related to the choice of boundary conditions for the solutions of the full S.E. These, in turn correspond to solutions of the asymtotic Hamiltonian, H_o. The solutions of H_o have already been

$$Y(\hat{r},\hat{R};\ J,M,j,\ell) = \sum_{m_j}\sum_{m_\ell} (\ j\ell J|m_j,\ M-m_\ell)\ Y^{\ell}_{m\ell}(\hat{R})\ \cdot\ Y^{j}_{mj}(\hat{r}) \tag{2.20}$$

For later purposes, it is convenient to define (Lester, 1975)

$$\phi_\alpha(\vec{r},\hat{R};J,M,n,j,\ell) = \frac{1}{r}\,\chi_{nj}(r)\ Y(\hat{r},\hat{R},J,M,j,\ell) \tag{2.21}$$

and to write the analogue of Eq. (2.19) as:

$$\Phi(\vec{r},\vec{R};\ E,J,M,n,j,\ell) = \frac{1}{R}\,U_{k\ell}(R)\ \cdot\ \phi_\alpha(\vec{r},\hat{R}) \tag{2.22}$$

Here the channel index α, defined by $\alpha = (n,j,\ell)$ has been introduced, and it would be appropriate to define the concept of channel as well. In the present context, one defines the system as being in channel α if it has the values of E,J,M,n,j,ℓ necessary to be described by Eq. (2.22). (In that sense, E,J,M should also be included in the channel label; however, the conservation properties of the Hamiltonian make this unnecessary. The reason for that will emergy shortly.) It is particularly important to note the difference between "state" and "channel". In the usual parlance, "state" corresponds to specifying (E,n,j). Thus one would expect the wavefunction for a state to

correspond to a superposition of channel functions like the one in Eq. (2.22) with differing values of J,M and ℓ.

To apply the coupled channel approach, one first notes that the eigenfunctions of H_o span not only the space of asymptotic solutions, but the space of scattering solutions of the full Hamiltonian as well. (Taylor, 1972). The spectrum of H consists, in general, of bound states (in which all three particles are bound), and scattering states in which at least one particle is asymptotically free. (For energies above the dissociation energy of the diatomic, one also has states with all three particles free.) The eigenfunctions of H_o span these scattering states. Therefore, one can expand any exact wavefunction for given values of E,J and M as:

$$\psi(\vec{r},\vec{R};E,J,M) = \sum_{\alpha} \frac{C_{\alpha}(R)}{R} \cdot \phi_{\alpha}(\vec{r},\hat{R}) \tag{2.23}$$

Because of the conservation properties of H, only the specified values of E,J, and M need be considered. The summation of Eq. (2.23) runs over the channel index $\alpha = (n,j,\ell)$. Now perhaps it is clear why the labels E,J,M were not included in the channel label. One should note that the justification for writing Eq. (2.23) is that the ϕ_{α}'s constitute a complete set. In particular the expansion is formally correct only if it includes <u>all</u> the internal states, even those lying in the B-C continuum. Of course, in the asymptotic region, one finds:

$$C_{\alpha}(R) = \begin{cases} a_{\alpha} \cdot u_{k\ell}(R), & \varepsilon_{nj} \leq E \\ 0, & \varepsilon_{nj} > E \end{cases} \tag{2.24}$$

Thus the energetically inaccessible, or "closed", channels carry no flux in the asymptotic region. However, they may be important in describing the wavefunction in the interaction region.

In practice, one disregards formal caveats and truncates the expansion at some convenient point. (Typically, one begins with a small basis set, say only the open channels, and then adds basis functions until the addition of one more set of channels causes a negligible difference in the calculated results.) Assuming the basis set has been truncated after the first N functions, one can write: (Lester, 1975).

$$\psi(\vec{r},R;\ E,J,M) = \sum_{\beta}^{N} \frac{C_\beta(R)}{R} \cdot \phi_\beta(\vec{r},\hat{R};\ J,M) \tag{2.25}$$

One then substitutes Eq. (2.25) into the full S.E.:

$$(H-E)\ \psi(\vec{r},\vec{R}\ ;\ E,J,M) = (H-E)\sum_{\beta} \frac{C_\beta(R)}{R}\ \phi_\beta(\vec{r},\hat{R};J,M) = 0 \tag{2.26}$$

One then takes matrix elements with each basis function in turn to obtain:

$$\sum_{\beta}(\phi_\alpha\,|H-E|\ \frac{C_\beta(R)}{R}\ \phi_\beta) = 0,\ \text{all}_\alpha \tag{2.27}$$

If one substitutes Eq. (2.5b) for H, and inserts the explicit dependence of the ϕ_α's on E,J, and M, one obtains the system of equations:

$$\left(\frac{d^2}{dR^2} - \frac{\ell_\alpha(\ell_\alpha+1)}{R^2} + k_\alpha^2\right) \cdot C_\alpha(R) = \frac{2\mu}{\hbar^2}\sum_{\beta} V_{\alpha\beta}(R;J) \cdot C_\beta(R) \tag{2.28}$$

where ℓ_α, k_α are the values appropriate for channel α, and

$$V_{\alpha\beta}(R;J) = \langle \phi_\alpha(\vec{r},\ \hat{R};\ J,M)|V_I(r,R,\gamma)|\ \phi_\beta(\vec{r},\hat{R};\ J,M)\rangle \tag{2.29}$$

Note that the M dependence of the ϕ_α's integrates out in Eq. (2.29).

Since k_α depends on E, and $V_{\alpha,\beta}$ depends on J, the radial expansion coefficients $C_\alpha(R)$ depend on E and J. (They do not depend on M. At this point, the only effect of different M states will be to introduce degeneracy factors of (2J+1) in certain expressions, notably the one defining the integral cross section.) It is convenient to note that each choice of values for E and J gives rise to a distinct set of coupled Eqs. (2.28), and thus to consider the solution Eqs. (2.28) for fixed values of E and J, and to suppress the somewhat cumbersome dependence on E and J.

Equations (2.28) represent a system of N coupled second-order linear differential equations (with first derivatives missing) of N unknowns. The system has 2N linearly independent solutions. The N irregular solutions are eliminated by the requirement that the wavefunction vanish at the origin. Thus, one expects N linearly independent regular solutions to Eqs. (2.28). One denotes these solutions by ψ_i, i running from one to N. Each of these solutions is defined in terms of an expansion like Eq. (2.23). It is convenient to reformulate the problem in matrix notation. One defines the solution vector $\vec{\psi}$ with i^{th} component ψ_i by:

$$\vec{\psi}(R) = \frac{1}{R}\,\vec{\phi}\cdot\underline{C}(R) \tag{2.30}$$

the matrix $\underline{C}$ can be shown to satisfy:

$$\sum_\beta \left(\delta_{\alpha\beta}\cdot\frac{d^2}{dR^2} + \delta_{\alpha\beta}k_\alpha^2\right)\cdot C_{\beta i}(R) = \sum_\beta\left(\frac{2\mu}{\hbar^2}V_{\alpha\beta}(R) + \delta_{\alpha\beta}\frac{\ell_\alpha(\ell_\alpha+1)}{R}\right)C_{\beta i}(R),\ \text{all}_{\alpha,i} \tag{2.31}$$

Equation (2.31) is just another version of Eq. (2.28). By making the obvious definitions, one may rewrite Eq. (2.31) in a more compact form:

$$(\underline{1} \cdot \frac{d^2}{dk^2} + \underline{k}) \cdot \underline{C} = \underline{U}_I \cdot \underline{C} \tag{2.32}$$

where $\underline{1}$ is the unit matrix and the label I indicates the interaction potential was used in Eq. (2.29). This, then completes the usual formulation of the N-coupled channel problem. In order to solve it, one may apply the method of Gordon (1969, 1971). A brief sketch of the method will be given here, the interested reader is referred to the literature for a more detailed treatment. The essence of the method can be stated as follows. If one is attempting to solve the Schroedinger Equation in a given region, one can consider subdividing the region into intervals sufficiently small so that the potential in each interval can be expanded in a rapidly convergent Taylor series about the mid-point. If one then considers the constant and linear terms as an approximating reference-potential, and the terms of order two and higher as a perturbation, one can write the solution to the reference problem explicitly in terms of Airy functions. The solution of the exact problem is then the reference solution plus a perturbation correction. If one assumes that the dominant corrections arise from the effect of the quadratic term, one can evaluate them analytically. One then chooses the intervals sufficiently small so that the corrections are less than the desired accuracy. By matching solutions and their derivatives at the boundaries of the intervals, one can construct a wavefunction which satisfies the S.E. to the desired degree of accuracy in the region

of interest.

To apply the method to the problem of interest here, one must first reformulate Eq. (2.32). One adds the term

$$\delta_{\alpha\beta}(2\mu\varepsilon_{nj}/\hbar^2)\ C_{\beta i}(R)$$

to both sides of Eq. (2.31). (The appropriate values of n and j are found from the channel label α.) One then obtains

$$\underline{1}\ (\frac{d^2}{dR^2} + E_o) \cdot \underline{C}(R) = \underline{U}(R) \cdot \underline{C}(R) \tag{2.33a}$$

where

$$U_{\alpha\beta} = (\phi_\alpha | \frac{2\mu}{\hbar^2} \cdot H + \frac{d^2}{dR^2} | \phi_\beta) \tag{2.33b}$$

and

$$E_o = 2\mu E/\hbar^2 \tag{2.33c}$$

The addition of the second term to the Hamiltonian in Eq. (2.33b) has the effect of concelling out the radial kinetic energy term for the relative translational motion. Thus, $U_{\alpha\beta}$ includes the total potential, both angular momentum terms, and the radial kinetic energy for internal motion.

One begins the solution of Eq. (2.33a) at a small enough value of R to guarantee that between the origin and that value of R the solution is smaller than the allowed error. (It will be recalled that the solution vanishes identically at the origin.) One then divides the remainder of the positive R-axis into intervals. At the left boundary of first interval the matrix C is set to zero and its derivative is taken to be a set of N linearly independent vectors.

One then propagates the solution in the following way. First one notes that the boundary conditions are specified in terms of initial conditions, i.e., one knows the value of the solution and its derivative at the left boundary of each interval. Assuming that one is on the ith interval, the problem is to propagate the solution through that interval. (The value of the solution and its derivative at the right boundary of the ith interval automatically specifies the "initial condition" for the $(i+1)^{th}$ interval.) Let $\bar{R}_i$ represent the mid-point of the ith interval. One then constructs a unitary matrix $\underline{M}_i$ such that:

$$\underline{\tilde{U}}(\bar{R}_i) = \underline{M}_i \, \underline{U}(R_i) \cdot \underline{M}_i^{\dagger} \tag{2.33a}$$

is diagonal. The effect of this transformation on Eq. (2.33a) is to replace $\underline{U}$ by $\underline{\tilde{U}}$. The solution matrix is also transformed:

$$\underline{\tilde{C}}_i = \underline{M}_i \, \underline{C} \, \underline{M}_i^{\dagger} \tag{2.34b}$$

Carrying out a Taylor series expansion on $\underline{\tilde{U}}$, one obtains:

$$\underline{\tilde{U}}(R) = \sum_n \frac{1}{n!} (R-\bar{R}_i)^n \, \underline{\tilde{U}}_n , \tag{2.35a}$$

where

$$\underline{\tilde{U}}_n = \frac{d^n}{dR^n} \underline{\tilde{U}}(R) \Big|_{R=\bar{R}_i} \tag{2.35b}$$

One then chooses the reference potential $\underline{\tilde{U}}_r$ as the diagonal matrix defined by:

$$(\underline{\tilde{U}}_r)_{\alpha\beta} = (\underline{\tilde{U}}_o)_{\alpha\beta} + \delta_{\alpha\beta} (R-\bar{R}_i) \, (\underline{\tilde{U}}_1)_{\alpha\beta} \tag{2.36a}$$

the first term in Eq. (2.36a) is the potential at the mid-point. It is diagonal by construction. The second term is explicitly diagonal by virtue of the Kronecker delta. The "perturbing" potential is everything not included in Eq. (2.36a). In keeping with the idea that the expansion in Eq. (2.35a) is rapidly convergent, one retains only the lowest order terms:

$$(\Delta\underline{\tilde{U}})_{\alpha\beta} = (\underline{\tilde{U}}-\underline{\tilde{U}}_r)_{\alpha\beta} \approx (1-\delta_{\alpha\beta}) \cdot (R-\bar{R}_i) \cdot (\underline{\tilde{U}}_1)_{\alpha\beta}$$

$$+ \delta_{\alpha\beta} \cdot \frac{1}{2}(R-\bar{R}_i)^2 \, (\underline{\tilde{U}}_2)_{\alpha\beta} \qquad (2.36b)$$

Since Eq. (2.36a) contains the diagonal first-order terms, the leading diagonal terms of the perturbation will be second order, whereas the leading off-diagonal terms will be first order.

The reference problem can be written:

all $_{\alpha\beta}$

$$\left(\frac{d^2}{dR^2} + E_o\right) \tilde{C}_{\alpha,n}(R) = [(\tilde{U}_o)_{\alpha\alpha} + (R-\bar{R}_i)\cdot(\tilde{U}_1)_{\alpha\alpha}] \cdot \tilde{C}_{\alpha,n}(R). \qquad (2.37)$$

This is a system of N uncoupled equations whose solution may be written as some linear combination of Airy functions:

$$\tilde{C}_{\alpha n} = Ai_\alpha(R) \cdot a_{\alpha n} + Bi_\alpha(R)\cdot b_{\alpha n}. \qquad (2.38)$$

Here $Ai_\alpha(R)$ and $Bi_\alpha(R)$ are the regular and irregular Airy functions appropriate to channel α, and $a_{\alpha n}$ and $b_{\alpha n}$ are constant coefficients whose specific values depend on the initial conditions for $\tilde{C}_{\alpha n}$.

One is interested, however, in the solution to the exact problem. Gordon (1964) shows that the exact solution may also be written in the form of Eq. (2.38), with the exception that now the expansion coefficients are no longer constant, but depend on R. One can estimate the change of a and b on the interval (R_ℓ, R_r) by:

$$\Delta a_{\alpha n} \approx -\frac{1}{W_\alpha} \int_{R_\ell}^{R_r} dR[B_{i_\alpha}(R) \cdot \sum_\beta (\Delta \tilde{U})_{\alpha\beta} \cdot \tilde{C}_{\beta n}] \tag{2.39a}$$

$$\Delta b_{\alpha n} \approx \frac{1}{W_\alpha} \int_{R_\ell}^{R_r} dR\ [A_{i_\alpha}(R) \cdot \sum_\beta (\Delta \tilde{U})_{\alpha\beta} \cdot \tilde{C}_{\beta n}], \tag{2.39b}$$

where the Wronskian W_α is defined by

$$W_\alpha = Ai_\alpha(R) \cdot Bi'_\alpha(R) - Ai'_\alpha(R) \cdot Bi_\alpha(R) \tag{2.39c}$$

It should be noted that Eqs. (2.39) contain a two-fold approximation. For exact equality to hold, one must use the complete perturbing potential, including all the higher-order terms neglected in Eq. (2.36b). Secondly, the $\tilde{C}_{\beta n}$ must be exact. The point then, is to make the interval size small enough so that the corrections given by Eqs. (2.39) are less than δ, the desired relative accuracy. One can determine the size of the first interval iteratively, and the size of subsequent intervals by:

$$\Delta R_{i+1} = \Delta R_i \cdot \min_\alpha \left(\delta \frac{|a_{\alpha n}| + |b_{\alpha n}|}{\max\ (|\Delta a_{\alpha n}|,\ |\Delta b_{\alpha n}|)}\right)^{1/3} \tag{2.40}$$

since the error varies roughly as the cube of the step size in this method.

In this way, by use of Eq. (2.38), the solution can be propagated to the right boundary of the ith interval. All that remains is establishing the initial condition on the $(i+1)^{th}$ interval. On

the $(i+1)^{th}$ interval one defines a new transformation M_{i+1}. One then has the analogues of Eqs. (2.34). Rewriting Eq. (2.34a) and its analogue, one has:

$$\underline{C} = \underline{M}_i^{\dagger} \underline{\tilde{C}}_i \underline{M}_i = M_{i+1}^{\dagger} \underline{\tilde{C}}_{i+1} \underline{M}_{i+1} \tag{2.41}$$

clearly,

$$\underline{\tilde{C}}_{i+1} = \underline{T}_i \underline{\tilde{C}}_i \underline{T}_i^{\dagger} , \tag{2.42a}$$

where

$$\underline{T}_i = \underline{M}_{i+1} \underline{M}_i^{\dagger} . \tag{2.42b}$$

To obtain the desired initial conditions, one evaluates $\underline{\tilde{C}}_i$ and its derivative at the right boundary of the ith interval and transforms them according to Eq. (2.42a). This then specifies the value of $\underline{\tilde{C}}_{i+1}$ and its derivative at the left boundary of the $(i+1)^{th}$ interval. One then propagates the solution on the $(i+1)^{th}$ interval as before.

The last difficulty is determining the S-matrix from the wavefunction. To do this, one assumes that the solution has been propagated into the asymptotic region. There, each element of the solution matrix looks like some linear combination of spherical Bessel functions (Gordon 1969):

$$c_{\alpha n} = j_{\alpha}(R) \cdot x_{\alpha n} + n_{\alpha}(R) \cdot y_{\alpha n} , \tag{2.43}$$

where

$$j_\alpha(R) = kR \cdot j_\ell(kR) \tag{2.44a}$$

$$n_\alpha(R) = kR \cdot n_\ell(kR) \tag{2.44b}$$

Here k and ℓ are the wavenumber and orbital angular momentum for channel α. j_ℓ and n_ℓ are the regular and irregular spherical Bessel functions of order ℓ. One can write Eq. (2.43) in matrix notation.

$$\underline{C} = j \cdot \underline{x} + \underline{n}\,\underline{Y} \tag{2.45a}$$

where

$$(\underline{j})_{\alpha\beta} = \delta_{\alpha\beta} j_\alpha(R) \tag{2.45b}$$

and

$$(\underline{n})_{\alpha\beta} = \delta_{\alpha\beta} n_\alpha(R) \tag{2.45c}$$

Ideally, one would like the asymptotic solution in the form:

$$\underline{C} = \underline{j} - \underline{n}\,\underline{k}^{-1/2}\underline{R}\,\underline{k}^{1/2} \tag{2.46}$$

where $\underline{k}$ is the wavenumber matrix appearing in Eq. (2.32) and $\underline{R}$ (also sometimes denoted as $\underline{K}$) is variously named the reactance, reaction, tangent, and Heitler matrix. It is the Cayley transform of the S-matrix (Taylor, 1972) and obeys the relation:

$$R = i(1-S)(1+S)^{-1}\ , \tag{2.47a}$$

which can be inverted to give:

$$S = (1+iR)(1-iR)^{-1} \tag{2.47b}$$

Using Eqs. (2.45a) and (2.46), one can show (Gordon, 1969) that R can be found by solution of:

$$(k^{1/2}X)^T R = (k^{1/2}Y)^T \tag{2.48}$$

where T denotes transpose of a matrix. This completes solution of the coupled channel problem for given E and J. One may define a partial cross-section for a given transition by (Lester, 1973)

$$\sigma^J_{n_1 j_1 \to n_2 j_2}(E) \quad \frac{\pi(2J+1)}{k_1^2(2j_{1+1})} \sum_{\ell_1,\ell_2} \delta_{n_1 n_2} \delta_{j_1 j_2} \delta_{\ell_1 \ell_2} - S^{J,E}_{n_1 j_1 \ell_1 \to n_2 j_2 \ell_2} \Big|^2 \tag{2.49}$$

Finally, one defines an integral cross-section as:

$$\sigma^{(E)}_{n_1 j_1 \to n_2 j_2} = \sum_J \sigma^J_{n_1 j_1 \to n_2 j_2}(E) \tag{2.50}$$

B. Classical S-Matrix Theory and Partial Averaging

This section gives a brief discussion of one formulation of classical-limit quantum mechanics, in effect a generalization of WKB theory to multi-dimensional problems. Also included is a description of the "partial averaging" method. This procedure allows one to treat classical-like internal modes (i.e., those strongly coupled to translation) in the spirit of quasi-classical Monte-Carlo while retaining semi-classical quantization (via the usual double-ended boundary conditions) for quantum-like modes, weakly coupled to translation.

Equations (2.49) and (2.50) of the previous section can be taken as the motivation of the present discussion. They express the quantity of interest, the cross-section, in terms of the S-matrix. Since the expressions are independent of the method used to calculate the S-matrix, any theory allowing the evaluation of S-matrix elements automatically allows one to compute the cross-section.

One such theory is the classical S-matrix formulation derived by Miller and co-workers. Using as a point of departure the Dirac view of quantum mechanics, i.e. a formulation stressing the importance of transformations, they have shown that one can derive an internally consistent formulation of classical-limit quantum mechanics given only two assumptions: (1) that the transformation element between a coordinate and its conjugate momentum be given by (in the Dirac notion):

$$\langle q|p\rangle = (2\pi i\hbar)^{-1/2}\, e^{iq\cdot p/\hbar}, \tag{2.51}$$

and (2), that integrals arising from transformations of coordinates or momenta be evaluated by the method of stationary phase, or the method

of steepest descents if there are no real points of stationary phase. It should be noted that assumption (1) is exactly equivalent to the uncertainty principle, and assumption (2) is the definition of "classical-limit".

The derivation of the theory will not be given here. It is the subject of two review articles by Miller, and the interested reader is referred to these for the details (Miller, 1974a, 1974b). The result pertinent to this discussion is how an S-matrix element for an inelastic transition may be approximated by use of classical trajectories. However, before the substance of the theory can be stated, it is first necessary to re-examine the system of interest and to re-cast the description of the scattering process into the language of classical mechanics.

To recap briefly, asymptotically at the beginning of the scattering event, the diatomic is in internal state (n_1,j_1) with energy $\varepsilon(n_1,j_1)$. The atom is "infinitely" far away (i.e., R sufficiently large that the interaction potential $V_I(r,R,\gamma)$ is negligible), approaching with translational energy $E_{tr} = E - \varepsilon(n_1 j_1)$ and orbital angular momentum ℓ_1, such that $|\vec{\ell}_1 + \vec{j}_1| = J$. The collision takes place, conserving total energy and angular momentum. The diatomic is now in state (n_2,j_2), and the atom recedes with translational energy $E_{tr} = E - \varepsilon(n_2,j_2)$ and orbital angular momentum ℓ_2. Of course, $|\vec{\ell}_2 + \vec{j}_2| = J$.

The above description of the collision process is given entirely in terms of quantum-mechanically observable quantities, as it must be, since one is dealing with a basically quantal process. The classical analogy is most easily made by use of action-angle variables. The

system is then described classically by four pairs of conjugate coordinates and momenta: (R,P_R), (q_n,n), (q_j,j), (q_ℓ,ℓ). The advantage of these variables is that the last three momenta, n,j,ℓ, are the classical analogues of the quantum numbers with the same labels. (Of course, as classical quantities, they are not restricted to integral values. This in fact is the motivation for the minor change in notation. The internal energy ε_{nj} of the last section now becomes $\varepsilon(n,j)$, since it seems natural to indicate integer anguments by subscripts and continuous arguments by the usual functional notation.) The transformation from this system of coordinates and momenta to the usual cartesian system is well-known (Miller, 1970, 1971, 1974a), and will not be given here. Thus the classical description of the asymptotic states consists of R "infinitely" large (i.e., large enough for the interaction potential to be negligible), P_R fixed by energy conservation, and the action variables set equal to their respective quantal (integer) values. It should be noted that the states are defined by exact values for the momenta, both intially and finally, but that the coordinates (i.e., position) variables are completely unspecified, except for a vague condition of R, whose purpose is to assure that the system is indeed in the asymptotic region. In fact, even this condition is based on an energetic consideration. The emphasis on energy and momentum is understandable, since the quantal description is in terms of energy and angular momentum eigenstates. The uncertainty principle requires that complete specification of momenta be accompanied by complete ignorance of the values of conjugate coordinates. Thus it is not surprising that the

classical analogy focuses on momenta and energy as well. Yet the coordinates, particularly the angles conjugate to the action variables, will be seen to play a crucial role in the theory.

Given the coordinate system defined above, one can write the classical Hamiltonian for the system (Miller, 1970) as:

$$H = (P_R^2 + \ell^2/R^2)/2\mu + \varepsilon(n,j) + V_I(r,R,\gamma). \tag{2.5a}$$

The variables r and γ are understood to be defined in terms of n,j,ℓ, and their conjugate angles. The exact expressions will not be given here (Miller, 1970), it should suffice to indicate the specific dependence:

$$r = r\ (n,j,q_n) \tag{2.52b}$$

$$\gamma = \gamma\ (n,j,\ell,q_n,q_j,q_\ell). \tag{2.52c}$$

The dynamical evolution of the system is given by Hamilton's equations of motion (Goldstein, 1950),

$$\dot{q}_i = \frac{\partial H}{\partial p_i}$$

$$\dot{p}_i = -\frac{\partial H}{\partial q_i}$$

where $\underline{i}$ denotes a particular pair of coordinate and conjugate momentum. It is instructive to consider the case in which the interaction potential is indentically zero. (Just as in the quantal description, the interaction potential goes to zero for large values of R. Thus one is looking at the classical analogue to the asymptotic states.)

If one defines the initial relative translational velocity v_1 and the impact parameter b by:

$$v_1 = (2(E-\varepsilon(n, j,))/\mu)^{1/2} \tag{2.54a}$$

and

$$b = \ell_1/(\mu v_1), \tag{2.54b}$$

then the trajectory functions are given by the following equations, assuming one chooses t = 0 to correspond to the distance of closest approach. (Doll and Miller).

$$n(t) = n_1 \tag{2.55a}$$

$$j(t) = j_1 \tag{2.55b}$$

$$\ell(t) = \ell_1$$

$$R(t) = (b^2 + v_1{}^2 t^2)^{1/2} \tag{2.55d}$$

$$P_R(t) = -\mu v_1 (1-b^2/R(t)^2)^{1/2} \tag{2.55e}$$

$$q_n(t) = q_{n_1} + \frac{\partial\varepsilon(n_1,j_1)}{\partial n_1} \cdot t \tag{2.55f}$$

$$q_j(t) = q_{j_1} + \frac{\partial\varepsilon(n_1,j_1)}{\partial j_1} \cdot t \tag{2.55g}$$

$$q_\ell(t) = q_{\ell_1} + \arctan(v_1 t/b) \tag{2.55h}$$

Inspection of Eqs. (2.55) will reveal two points. First, in order to describe an asymptotic state classically, one must specify the values of

$$(q_{n_1}, q_{j_1}, q_{\ell_1}, E, J, n_1, j_1, \ell_1).$$

The variable J does not appear in Eqs. (2.55), but its value is required in the computation of γ, and thus if the interaction potential is non-zero, J must be specified. Second, in the asymptotic region, the values of n,j and ℓ are constant, as expected, since their conjugate coordinates are cyclic (i.e., do not appear) in the asymptotic Hamiltonian. The effect of the interaction potential is to introduce the angle variables into the Hamiltonian, thus destroying the time invariance of the action variables. Further, one should recall that the interaction potential is explicitly a function of R,r, and γ; however, the last two variables depend in turn on all the action-angle variables. Thus, the presence of the interaction potential couples all the modes. For example, the term $\frac{\partial V_I}{\partial q_n}$, which appears in Hamilton's equation for $\dot{n}$, is a function of R,n,j,ℓ, q_ℓ and q_ℓ. The presence of this term, then, couples the vibrational motion to rotation and translation. This, of course, is completely analogous to the situation in the coupled channel problem, where the coupling was also seen to arise from the effect of the interaction potential. (See Eqs. (2.28) and (2.29).)

At this point, one is finally able to state the so-called classical S-matrix formula. First one recognizes that the classical analogue of a quantum scattering event going from channel (n_1, j_1, ℓ_1) to

channel (n_2, j_2, ℓ_2) at fixed J and E is a trajectory starting in the asymptotic region at time t_1 and ending again the asymptotic region at time t_2, such that:

$$n(t_1) = n_1 \tag{2.56a}$$

$$j(t_1) = j_1 \tag{2.56b}$$

$$\ell(t_1) = \ell_1 \tag{2.56c}$$

and

$$n(t_2) = n_2 \tag{2.56d}$$

$$j(t_2) = j_2 \tag{2.56e}$$

$$\ell(t_2) = \ell_2 \tag{2.56f}$$

Equations (2.56) are examples of the so-called double-ended boundary conditions, in which the boundary values are specified partially at the beginning of the trajectory and partially at the end. In practice, to evaluate a trajectory numerically, one must specify initial conditions for all the variables. This situation leads to the root search problem. One must find values of q_{n_1}, q_{j_1}, and q_{ℓ_1} such that, together with the initial conditions in Eqs. (2.56a, b, c), they define a trajectory satisfying Eqs. (2.56d, e, f). If the action variables are initially fixed to the values defined by Eqs. (2.56a, b, c), one can consider their final values to be functions of the initial values of the angle variables:

$$n_2 = n_2(q_{n_1}, q_{j_1}, q_{\ell_1}) \tag{2.57a}$$

$$j_2 = j_2(q_{n_1}, q_{j_1}, q_{\ell_1}) \tag{2.57b}$$

$$\ell_2 = \ell_2(q_{n_1}, q_{j_1}, q_{\ell_1}) \tag{2.57c}$$

The desired angle variables are the roots (i.e. solution) of the equations resulting from equating the expressions in Eqs. (2.57a, b, c) to the desired final boundary values defined by Eqs. (2.56d, e, f). (One should note that q_{n_1}, for example, is <u>not</u> the value of q_n at time t_1. Rather, since the system is in the asymptotic region, $q_n(t_1)$ is calculated from q_{n_1} by use of Eq. (2.55f). The reason one chooses q_{n_1} rather than $q_n(t_1)$ in Eq. (2.57a) is that q_{n_1} is time independent, where as $q_n(t_1)$ does have an admittedly simple dependence on t_1. Similar remarks apply to q_j and q_ℓ. Thus as long as t_1 and t_2 are chosen so the system is in the asymptotic region at both these points in time (so that Eqs. (2.55) and (2.56) hold), the root search problem defined by Eqs. (2.57), and its solution, do not depend on the values of t_1 or t_2. These remarks have been included to clarify a possible source of confusion in the notation, since for the action variables the subscript 1 can be taken to denote their values at time t_1, and the subscript 2 to denote their value at time t_2).

Once one finds the desired trajectory one can compute the S-matrix element by the formula:

$$S_{n_2 j_2 \ell_2 \; n_1 j_1 \ell_1}^{(J,E)} = \frac{e^{\frac{1}{\hbar}\int_{t_1}^{t_2} dt \; (R\cdot\dot{P}_R + q_n\cdot\dot{n} + q_j\cdot\dot{j} + q_\ell\cdot\dot{\ell})}}{\left((2\pi i\hbar)^3 \cdot \left| \frac{\partial(n_2, j_2, \ell_2)}{\partial(q_{n_1}, q_{j_1}, q_{\ell_1})} \right| \right)^{1/2}} \tag{2.58}$$

Of course, Eqs. (2.57) may have multiple solutions, i.e., there may be more than one trajectory satisfying the double-ended boundary conditions imposed by Eqs. (2.56). In this case, the S-matrix element is the sum over all such trajectories of expression (2.58). This of course gives rise to interference effects; (just as in the semiclassical theory of elastic scattering, if $b(\theta)$, i.e., the inverse of the deflection function, is multivalued.) It is also possible that Eqs. (2.57) have no real solutions. Then it is necessary to look at complex solutions (Miller and George, 1972). If the integral in Eq. (2.58) is real, as it will be if the trajectory function are real, then the exponential has a purely imaginary argument and thus acts as a phase factor. If on the other hand, the integral is complex, then its imaginary part becomes the real part of the exponential's argument, leading to exponential damping. Thus one would expect the contribution to an S-matrix element arising from complex solutions to Eq. (2.57) to be much smaller than any corresponding contribution from real solutions. This means that complex trajectories are important only in so-called "classically forbidden" problems, i.e., those for which Eqs. (2.57) have no real solutions. (The easiest example to point out is the case of barrier penetration or tunnelling. In the present case, the

"forbiddenness" can be viewed as follows. For a transition to be classically allowed, it must be allowed by energy conservation, and there must be trajectories which explore regions where the translation-vibration coupling, let's say, is sufficiently strong to allow the transition to take place. It is possible that these regions of strong coupling are energetically inaccessible in the energy range chosen. Thus in order for the transition to take place, the system must tunnel into a classically forbidden region of strong coupling, where the transition is dynamically allowed.) Of course, there may be multiple complex solutions. By the same token, one need only consider the solution which leads to the smallest imaginary part for the integral in Eq. (2.58). All other solutions will be more strongly damped and hence make negligible contributions by comparison.

In order to compute the cross section, one merely substitutes Eq. (2.58) into Eqs. (2.49) and (2.5 of the previous section. The final expression can be written: (for an inelastic transition)

$$\sigma_{n_2 j_2 \leftarrow n_1 j_1}(E) = \frac{\pi}{k_1^2(2j_1+1)} \sum_J (2J+1) \sum_{\ell_1} \sum_{\ell_2} \left| \sum_r \frac{e^{\frac{-i}{\hbar}\phi_r}}{((2\pi i\hbar)^3 D_r)^{1/2}} \right|^2 \tag{2.59a}$$

where the sum over r indicates a sum over all solutions of the root search problem defined by Eqs. (2.57), and ϕ and D are defined for the rth trajectory by:

$$\phi = \int_{t_1}^{t_2} dt \; (R\cdot\dot{P}_R + q_n\cdot\dot{n} + q_j\cdot\dot{j} + q_\ell\,\dot{\ell}), \tag{2.59b}$$

$$D = \left| \frac{\partial(n_2, j_2, \ell_2)}{\partial(q_{n_1}, q_{j_1}, q_{\ell_1})} \right| \tag{2.59c}$$

If one considers calculating all possible cross sections from $n_1 = 1$, $j_1 = 0$ thru 6 to $n_2 = 0$, $j_2 = 0$ thru 8 for, say H_2 + He, where one can expect all partial waves out to J = 60 to contribute, it is easy to show that the calculation would require about 24,000 root searches if Eq. (2.59a) were used as is. It is with the hope of reducing this prohibitively laborious chore that one introduces the idea of partial averaging. (Miller and Raczkowski, 1973)

The problem with Eq. (2.59a) is that it faithfully keeps track of interference effects in individual S-matrix elements and then sums the result over a large number of terms to compute the cross section. (The number of terms varies with the transition; in the example of H_2 + He quoted above, there are 60 terms in $\sigma_{00\leftarrow 10}$ and 1200 terms in $\sigma_{08\leftarrow 16}$.) It has been pointed out (Miller, 1971) that if a sum contains more than ten or twenty terms, one may be quite certain that interference effects in the summand will be quenched. Secondly, because of the large number of terms in the sums, it would be in keeping with the semiclassical spirit to replace the sums by integrals.

Perhaps the conceptually simplest way of arriving at the partially averaged formula for the cross sections is to consider a cross section of the form $\sigma_{n_2\leftarrow n_1 j_1}$. This merely introduces a sum over j_2 into Eq. (2.59a). If one now neglects interference and replaces the sums over j_2, ℓ_2, ℓ_1, and J by integrals, the expression becomes:

$$\sigma_{n_2 \leftarrow n_1 j_1}(E) =$$

$$\frac{\pi}{k_1^2(2j_1+1)} \int_0^\infty d(J^2) \int_{|J-j_1|}^{(J+j_1)} d\ell_1 \int_{|J-j_2|}^{(J+j_2)} d\ell_2 \int_0^\infty dj_2 \frac{e^{\frac{-2}{\hbar}\,\mathrm{Im}(\phi)}}{(2\pi\hbar)^3 D} \tag{2.60}$$

where ϕ and D are defined by Eqs. 2.59b, c). One then changes variables of integration from j_2 and ℓ_2 to q_{j_1} and q_{ℓ_1}. The Jacobian of the transformation partially cancels D (see Eq. 2.59c), and one obtains finally:

$$\sigma_{n_2 \leftarrow n_1 j_1}(E) =$$

$$\frac{\pi}{k_1^2(2j_1+1)} \int_0^\infty d(J^2) \int_{|J-j_1|}^{(J+j_1)} d\ell_1 \int_0^1 d\left(\frac{q_{j_1}}{2\pi}\right) \int_0^1 d\left(\frac{q_{\ell_1}}{2\pi}\right) \frac{e^{\frac{-2}{\hbar}|\mathrm{Im}(\phi)|}}{2\pi\hbar^3 \left|\frac{\partial n_2}{\partial q_{n_1}}\right|} \tag{2.61}$$

In order to apply this formula, one evaluates the integrals by Monte Carlo: for each integration variable one randomly chooses a value from its range of integration, one then evaluates the integrand at this "point" (i.e., for those values of the integration variables), one repeats this process N times. The value of the integral is then taken to be the arithmetic average of the integrand evaluated at the N points. It should be noted that evaluation of the integrand in Eq.

(2.61) still involves satisfying a double-ended boundary conditions. With n_1, j_1 and the total energy specified, the Monte Carlo procedure supplies initial conditions for all but one variable. The prescription for finding q_{n_1} is that its value must lead to the vibrational action variable having the desired final value n_2. If one is computing $\sigma_{0\leftarrow 1,j_1}$, say, this condition can be written:

$$n_2(q_{n_1}) = 0. \tag{2.62}$$

Thus the partial averaging formula does indeed simplify the calculational task in two ways. First it reduces the dimensionality of root search problem. (The importance of this will emerge from the discussion in the chapter on calculations.) Second, it reduces the number of root searches which must be performed. The evaluation of the integral in Eq. (2.61) by Monte Carlo basically consists of finding N trajectories which start in state (n_1, j_1) and end in some state (n_2, j_2); one places no restriction on j_2. Associated with each trajectory is some transition probability, found by evaluating the integrand in Eq. (2.61). In order to find the total cross section to n_2, one sums this probability over all N trajectories. But since one knows all the trajectory functions for each trajectory, one could approximate the cross section to (n_2, j_2) for each j_2 by just summing over those trajectories which have final j values between (j_2-1/2) and (j_2+1/2). (In the original formulation of the problem as expressed by Eq. 2.59a), j_2 and ℓ_2 were guaranteed to be integers by the boundary conditions in Eqs. (2.56e, f). Use of the partial averaging formula only guarantees

that the boundary condition on n_2 is satisfied; j_2 and ℓ_2 can have any non-negative real value.) Similarly, the differential cross section can be approximated by dividing the interval $(0, \pi)$ into increments of $\Delta\theta$, and computing the differential cross section in each increment by summing over only those trajectories which have scattering angles in the desired range.

This of course means that N, the number of Monte Carlo points used, will depend on how detailed is the information being sought. In the case of $H_2 + Li^+$, where differential cross sections were obtained, 1000 points were used. In the H_2 + He study, where only the integral cross sections were of interest, and these were required at several energies, one hundred points were used for each initial state and energy. Thus, the calculation which would require 24,000 three-dimensional root searches if Eq. (2.59a) were used was reduced to one requiring only 400 one-dimensional root searches by use of the partial averaging formula. This amounts to a saving of effort of several orders of magnitude, where one considers the relative facility of 1-D over 3-D searches.

C. Rate Constants and Relaxation Times

This section gives a discussion of how one would use the cross section data, derived in the previous two sections, to calculate the rate constants for the specific quantum state transitions, and eventually utilize this information to characterize the relaxation, i.e., approach to equilibrium, of a perturbed system. The topics of this section are straightforward and well-documented in the literature. Thus again, the discussion will be brief, all proofs will be omitted, and the reader interested in further details will be referred to the literature.

If one considers a bimolecular process of the form

$$H_2(n_1,j_1) + He(v_1) \rightarrow H_2(n_2,j_2) + He(v_2) \qquad (2.62)$$

(The meaning of Eq. (2.62) is that H_2 in the internal state (n_1,j_1) collides with He approaching asymptotically with relative velocity v_1, energy transfer takes place, and H_2 emerges in state (n_2,j_2), and He recedes with relative velocity v_2.), one can write the rate constant for the process as (Weston and Schwarz, 1972):

$$k_{2\leftarrow 1} = v_1 \cdot \sigma_{2\leftarrow 1} \qquad (2.63a)$$

where the subscripts 1 and 2 are now used as generic labels for the initial and final states, respectively, and σ is the relevant cross section, <u>i.e.</u>,

$$\sigma_{2\leftarrow 1} = \sigma^{(E)}_{n_2 j_2 \leftarrow n_1 j_1} \qquad (2.63b)$$

in the notation of the previous two sections, where the total energy E is given by:

$$E = \frac{\mu v_1^2}{2} + \varepsilon_{n_1 j_1} = E_{tr} + \varepsilon_{n_1 j_1}. \tag{2.63c}$$

thus, $\sigma_{2\leftarrow 1}$ can be considered a function of the initial relative velocity or translational energy.

Of course, if the system is characterized by a distribution of relative velocities, $\rho(v)$, then the rate constant is the average of Eq. (2.63a) over the distribution:

$$k_{2\leftarrow 1} = \int_o^\infty v_1 \sigma_{2\leftarrow 1} \rho(v_1) dv_1. \tag{2.64}$$

The most common case is where $\rho(v)$ is the Maxwell-Boltzmann velocity distribution characteristic of some translational temperature T. The function $\rho_T(v)$ is then given by:

$$\rho_T(v) = 4\pi \left(\frac{\beta\mu}{2\pi}\right)^{3/2} v^2 e^{-\frac{\beta\mu v^2}{2}} \tag{2.65}$$

In order to avoid confusion between the rate constant and Boltzmann's constant, both of which are traditionally designated by k, it is convenient to define the quantity by:

$$\beta = (k_B T)^{-1} \tag{2.66}$$

where k_B is Boltzmann's constant. It is trivial to show that if one performs the change of variable:

$$\varepsilon = \beta \cdot E_{tr} = \frac{\beta\mu v^2}{2} \tag{2.67}$$

Eq. (2.64) with $\rho(v_1)$ defined by Eq. (2.65) becomes:

$$k_{2\leftarrow 1}^{(T)} = \langle V\rangle_T \cdot \langle\sigma_{2\leftarrow 1}\rangle_T, \tag{2.68a}$$

where

$$\langle V\rangle_T = \left(\frac{8}{\pi\beta\cdot\mu}\right)^{1/2} \tag{2.68b}$$

and

$$\langle\sigma_{2\leftarrow 1}\rangle_T = \int_0^\infty \varepsilon\cdot\sigma_{2\leftarrow 1}(\varepsilon)\cdot e^{-\varepsilon}d\varepsilon. \tag{2.68c}$$

The function $\sigma_{2\leftarrow 1}(\varepsilon)$ is defined in analogy with Eqs. (2.63b, c) by:

$$\sigma_{2\leftarrow 1}(\varepsilon) = \sigma_{n_2 j_2 \leftarrow n_1 j_1}((\varepsilon/\beta) + \varepsilon_{n_1 j_1}) \tag{2.68d}$$

Having defined the rate constant, one can show that the rate of transition from state one to state two is given by:

$$R_{2\leftarrow 1} = k_{2\leftarrow 1} \cdot [He] \cdot [H_2(n_1, j_1)], \tag{2.69}$$

where [He], for example, stands for the concentration of He. One wishes at this point to discard the generic notation for initial and final states and to consider some specific ordering of the internal states of H_2, now labelled one through N. (the exact ordering is immaterial,) so that the subscript $\underline{i}$ refers to some definite state. One can then define a population vector $\vec{\eta}(t)$, whose i^{th} component, $\eta_i(t)$, is the instantaneous population of the ith internal state of H_2 at time t. It is convenient to impose the normalization condition:

$$\sum_i \eta_i = 1. \tag{2.70}$$

The variable $\eta_i(t)$ is then the population fraction in state i at time t. Of course, the system tends toward equilibrium and in the limit of infinite time, the population fractions tend to their equilibrium values. These can be denoted as p_i, for later reference, and they are given by the usual relation:

$$\lim_{t \to +\infty} \eta_i(t) = p_i = \frac{g_i e^{-\beta\varepsilon_i}}{\sum_j g_j e^{-\beta\varepsilon_j}} \tag{2.71}$$

where g_i and ε_i are the degeneracy and energy of the ith internal state.

The purpose, however, is to describe the time evolution of a perturbed system for all times t, not merely in the infinite limit. Thus $\eta(t)$ must be considered an arbitrary vector with non-negative components, satisfying Eq. (2.70). At any point in time, the populations must satify the relation: for all i,

$$\dot{\eta}_i = \sum_{j \neq i} R_{i \leftarrow j} - \sum_{j \neq i} R_{j \leftarrow i}. \tag{2.72}$$

Equation (2.72) is merely the consequence of Eq. (2.70), which in turn follows from the conservation of matter. Equation (2.70) requires that no particles be gained or lost by the system as a whole. Thus the gains in the population of level <u>i</u> are caused only by transitions from other states, and losses only by transition <u>to</u> other states. Eq. (2.72) expresses the net change in level <u>i</u> as gains minus losses.

(Oppenheim, Shuler, and Weis, 1967). Using Eq. (2.69) for the rate and letting ρ = [He], one can rewrite Eq. (2.72) in the more convenient matrix notation as the so-called Master Equation:

$$\dot{\vec{\eta}}(t) = \rho \cdot \underline{K} \cdot \vec{\eta}(t), \tag{2.73}$$

where the matrix $\underline{K}$ is defined by:

$$K_{ij} = \begin{cases} k_{i \leftarrow j}, & i \neq j \\ -\sum_{\ell \neq i} k_{\ell \leftarrow i}, & i = j \end{cases} \tag{2.74}$$

the differential Eq. (2.73) has the formal solution:

$$\vec{\eta}(t) = e^{\underline{K} \rho t} \cdot \vec{\eta}(0). \tag{2.75a}$$

It is customary to incorporate the scalar factor ρ into t and write

$$\vec{\eta}(t) = e^{\underline{K} t} \cdot \vec{\eta}(0). \tag{2.75b}$$

One now seeks to diagonalize $\underline{K}$, since this will lead to a more readily interpretable expression for the time behavior. The diagonalization is usually carried through in two steps (Rabitz and Zarur, 1975). One first symmetrizes the matrix $\underline{K}$. Since at equilibrium $R_{i \leftarrow j}$ equals $R_{j \leftarrow i}$, it follows immediately by use of Eqs. (2.69) and (2.74) that

$$K_{ij} = \frac{p_i}{p_j} \cdot K_{ji}. \tag{2.76}$$

This is the so-called detailed balance relationship. Defining the matrix T_1 by:

$$(T_1)_{ij} = \delta_{ij}\, p_i^{1/2} \tag{2.77}$$

one can show that the transformation:

$$\underline{K}_1 = \underline{T}_1^{-1} \cdot \underline{K} \cdot \underline{T}_1 \tag{2.78}$$

yields a transformed matrix $\underline{K}_1$ which is symmetric. The symmetric matrix $\underline{K}_1$ can now be diagonalized by the transformation T_2, i.e.:

$$\underline{\lambda} = \underline{T}_2^{-1} \cdot \underline{K}_1 \cdot \underline{T}_2 \tag{2.79a}$$

where

$$(\underline{\lambda})_{ij} = \delta_{ij} \cdot \lambda_i \tag{2.79b}$$

The variable λ_i denotes the ith eigenvalue of the rate matrix. It follows from Eqs. (2.70) and (2.76) that the eigenvalues are all real and can be ordered as follows (see Oppenheim, et al., 1967):

$$0 = \lambda_1 \geqslant \lambda_2 \geqslant \ldots \geqslant \lambda_N \tag{2.80}$$

Finally, defining the matrix $\mathring{M}$ by:

$$\underline{M} = \underline{T}_1 \cdot \underline{T}_2, \tag{2.81}$$

one can write

$$\underline{K} = \underline{M}\, \underline{\lambda}\, \underline{M}^{-1}, \tag{2.82}$$

and Eq. (2.79b) can be rewritten as:

$$\vec{\eta}(t) = M\, e^{\underline{\lambda} t}\, M^{-1} \cdot \vec{\eta}(0) \tag{2.83a}$$

or equivalently,

for all i,

$$\omega_i(t) = e^{\lambda_i t}\, \omega_i(0), \tag{2.83b}$$

where the transformed population vector $\vec{\omega}$ is given by:

$$\vec{\omega} = \underline{M}^{-1} \cdot \vec{\eta} \tag{2.83c}$$

Equation (2.83b) is obtained from its predecessor by left-multiplying both sides by M^{-1}; this mathematically simple operation, however, corresponds to a conceptually profound shift in perspective. Whereas Eq. (2.83a) retains the same basis set as its ultimate antecedent, Eq. (2.75b), Eq. (2.83b) in essence describes the results of a change of basis. This change of basis corresponds to a very marked change in how the system is being described. In order to amplify these remarks, one must look closely at the fundamental underpinnings of Eqs. (2.75) and (2.83).

In order to define the vector $\vec{\eta}$, one takes the elements of the standard basis set $\{\varepsilon_i\}$ to correspond in turn to the presence of one particle in the ith level. (The ith standard basis vector is just the vector with 1 in the ith place and zeroes elsewhere, for example, $\{\hat{i}, \hat{j}, \hat{k}\}$ is the standard basis set for Euclidean three-space.) One then defines the components of $\vec{\eta}$ by

$$\vec{\eta} = \sum_i \eta_i \, \varepsilon_i . \tag{2.84}$$

Thus $\vec{\eta}$ defines the system in terms of the populations of individual levels, and the rate matrix $\underline{K}$ describes the relaxation of the system in terms of transitions between individual levels. This, of course, is the most intuitive formulation.

To obtain Eq. (2.83b), on the other hand, one uses the transformed basis set $\{\vec{u}_i\}$, whose elements are given by:

$$\vec{u}_i = \underline{M} \cdot \vec{\varepsilon}_i \tag{2.85}$$

where $\underline{M}$ is defined by Eq.(2.81). The system is described by the population vector $\vec{\omega}$, whose components obey:

$$\vec{\omega} = \sum_i \omega_i \cdot \vec{u}_i , \tag{2.86}$$

and they are related to the components of $\vec{\eta}$ by Eq. (2.83c). Of course, since $\underline{M}$ diagonalizes $\underline{K}$, the $\vec{u}_i$'s are just the eigenvectors of $\underline{K}$. One can show easily that $\vec{u}_1$ is just the equilibrium population distribution. Since the corresponding eigenvalue λ_1 is zero, Eq. (2.83b) shows that ω_1 is time independent. The other eigenvectors correspond to deviations from equilibrium which die away with characteristic rates λ_i. One is now describing the relaxation of the system in terms of concerted processes (i.e., linear combinations of individual transition,) which lead to uncoupled equations for the time dependence. Perhaps the most useful analogy is the case of the internal motions of polyatomic molecules, where one transforms from the usual cartesian coordinates of each atom to the normal coordinates of the molecule as a whole (i.e.

concerted motions of the atoms.) In the process, one greatly simplifies the equations of motion by transforming away the lowest-order coupling terms. In the present case as well, one goes from a myopic description in terms of transitions between individual levels to an overall view of the relaxation of the system at large.

Equation (2.83b) leads naturally to the idea of relaxation modes and times. If one defines the relaxation time of the ith mode (i.e., the one corresponding to the population imbalance described by $\vec{u}_i$) as:

$$\tau_i = -\lambda_i^{-1} , \tag{2.87}$$

its component clearly goes to zero as:

$$\omega_i(t) = e^{-t/\tau_i} \cdot \omega_i(0).$$

If the population imbalance at time zero is described by only one mode, the approach to equilibrium will be a simple exponential function of time. This is called "pure mode relaxation." However, if several modes are initially present, the time dependence will be a sum of exponentials. Of course, if the eigenvalues of the rate matrix are well separated, one would expect that for long enough times, only the contribution from the mode with the longest relaxation time (i.e., slowest rate) would be significant. Because of the ordering in Eq. (2.80), the longest relaxation time is τ_2. This quantity should then be observable, even if it is impossible to prepare the system initially in the pure mode $\vec{u}_2$.

III. CALCULATIONS AND RESULTS

This chapter concerns itself with the actual application of the theory discussed previously to two real systems, H_2-He and H_2-Li^+. The material will be presented in chronological order, after a few preliminary remarks to set the stage. The calculations to be described include use of the classical-limit method on both systems, and a coupled-channel calculation on H_2-He. The H_2-He studies are technically less interesting, since the coupled-channel calculation was routine, employing well-known procedures, and the classical-limit calculation merely involved application of the methods developed during the H_2-Li^+ study. The H_2-Li^+ work, then, is more interesting from the technical point of view, since it entailed the development of the current methods of applying classical-limit theory to non-reactive, three-dimensional systems. Consequently its description occupies a prominent place in this chapter. On the other hand, the parallel calculations of Rabitz and Zarur (1975), McGuire and Toennies (1975), and Alexander (1975), as well as the experimental work of Audibert, Joffrin and Ducuing, lend special pertinence to the results of H_2-He relaxation study.

Before proceeding to a discussion of techniques used to circumvent difficulties in applying the classical-limit method, it seems worthwhile to restate the nature of the method and give a more detailed account of the difficulties. As will be recalled from Section II.B, the partially-averaged classical limit method calls for finding N trajectories whose initial conditions are given as follows:

E, n_1 and j_1 are specified in the cross-section to be calculated, J, ℓ_1, q_{j_1} and q_{ℓ_1} are initialized by the Monte Carlo procedure, and q_{n_1} is chosen to satisfy the requirement:

$$n_2(q_{n_1}) = n_2. \tag{3.1}$$

Associated with each trajectory is a probability (or weighting) factor, given by the formula of Eq. (2.61). In order to compute the cross-section, one averages this probability over all N trajectories.

Now, to consider explicitly the case of complex trajectories, one must begin with Eq. (2.59a), with the explicit summing of the S-matrix elements. The corresponding complex boundary conditions for the trajectories leading to S-matrix elements are the following: the real parts are fixed as before (see Eqs. (2.56) and (2.56)), except that the arguments are now complex, and imaginary parts are set equal to zero. The partial-averaging method again allows one to remove the restrictions on the real parts of j_2 and ℓ_2 by averaging over q_{j_1} and q_{ℓ_1}, and the boundary conditions for the Monte Carlo trajectories become

$$\mathrm{Re}\, n_2(\mathrm{Re}\, q_{n_1}, \mathrm{Im}\, q_{n_1}, \mathrm{Im}\, q_{j_1}, \mathrm{Im}\, q_{\ell_1}) = n_2 \tag{3.2a}$$

$$\mathrm{Im}\, n_2(\mathrm{Re}\, q_{n_1}, \mathrm{Im}\, q_{n_1}, \mathrm{Im}\, q_{j_1}, \mathrm{Im}\, q_{\ell_1}) = 0 \tag{3.2b}$$

$$\mathrm{Im}\, j_2(\mathrm{Re}\, q_{n_1}, \mathrm{Im}\, q_{n_1}, \mathrm{Im}\, q_{j_1}, \mathrm{Im}\, q_{\ell_1}) = 0 \tag{3.2c}$$

$$\mathrm{Im}\, \ell_2(\mathrm{Re}\, q_{n_1}, \mathrm{Im}\, q_{n_1}, \mathrm{Im}\, q_{j_1}, \mathrm{Im}\, q_{\ell_1}) = 0 \tag{3.2d}$$

(It will be recalled that Re q_{j_1} and Re q_{ℓ_1} are specified for each trajectory by the Monte Carlo procedure.) Thus, while for real trajectories the partial-averaging method reduces the dimensionality of the root search from 3-D to 1-D, for complex trajectories the reduction is less profound, from 6-D to 4-D. Thus the first difficulty is that one must still perform a multi-dimensional root search at each Monte Carlo point.

The second complication is the running of the complex trajectories, i.e., the numerical integration of the equations of motion along a complex time path, beginning with complex initial conditions. This procedure presents a two-fold difficulty. First, because of the trajectories' ability to tunnel, they are sensitive to the global features of the potential. The potential for real systems is usually known in terms of ab initio values at a given set of points. One then performs an analytic (in the complex analysis sense) fit to the points to define the potential on the positive real axis and then continues this fit to define the potential in the complex plane. Thus, different fits to the same set of ab initio values will have different continuations in the complex plane. (Of course, if the potential were analytically known for real values of its arguments, the continuation into the complex plane would be unique.) The consequence is that for real trajectories, if one can show that the system is confined classically to some region of space, one need only concern oneself with fitting the potential locally. The behavior of the fitting function in the classically inaccessible

region is immaterial. (Fits are usually constructed to extrapolate properly in the translational coordinates; however, in describing the vibrational dependence the fit is often only good within a bohr radius or so from the equilibrium position, and the extrapolation properties in the vibrational coordinate are seldom considered.) For complex trajectories, this is no longer true. The trajectories can tunnel into all regions of space. Thus the fitting function must have the correct global character as well as representing the potential correctly in the region of the *ab initio* points. Unfortunately, while the occurrence of unreasonable values for regions of the real axis can be used to screen out unacceptable fitting functions, the converse is not necesserily true. Correct behaviour on the real axis does not necessarily lead to desirable characteristics in the analytic continuation. The question of *a priori* determining the suitability of some fitting form is at present an open one. The suitability can only be determined *a posteriori* by looking at the results of trajectories run on that potential surface.

The second difficulty has to do with the vibrational motion. For real trajectories, the motion is oscillatory, *i.e.* moving back and forth along the real axis between the turning points. For present purposes, the case of oscillations sinusoidal in time can be considered. For complex trajectories, the motion will now trace an ellipse in the complex plane with the turning points (now complex) as its foci. The motion is still sinusoidal, but the argument of the sine, *i.e.*, the time, is now complex. The imaginary part of the time imparts exponential growth to the oscillation.

Thus, even with an entirely reasonable interaction potential, trajectories may not complete satisfactorily, because of unbounded vibrational motion in the oscillator. Restricting the time to real values is not possible, since that would be equivalent to allowing only real trajectories, thus vitiating the classical-limit method's ability to deal with classical forbidden processes. One is in the paradoxical situation where the feature allowing the method to broaden its scope to classical forbidden cases is also the ultimate source of difficulties in the application of the method.

Fortunately, the problem of the vibrational motion is amenable to solution. Classical S-matrix theory requires only that the real part of the difference between a trajectory's starting time and end time tend to infinity. There is no restriction on the actual time path followed. In principle, given the trajectory's initial conditions, all time paths with the same end points must lead to the same final values for the trajectory functions. In practice, some paths will lead to numerically more stable trajectories than others. Thus one must choose a path through the complex time plane such that the vibrational motion builds up enough complex character to overcome the "forbiddenness" of the desired transition, but not sufficient to cause unbounded motion. Clearly, the choice of such a path may require some finesse.

In summary then, the success of the classical-limit method is contingent upon two interrelated criteria: (1) being able to run trajectories (that is, given the initial values for all variables,

being able to perform a stable, convergent numerical integration of the equations of motion), and (2) being able to find roots (that is, given a set double-ended boundary conditions, being able to find values for the initially unspecified variables such that the final conditions of the problem are satisfied). The two requirements are interrelated because the typical root-search algorithm uses the results of its previous four or so guesses to give a new, and it is hoped, more accurate guess for the root. To tell how well the root searcher is doing one must run the trajectory with the current guess as the initial condition. The error (i.e., the computed final values minus the desired final values,) is used in determining the next guess. If at some point the root searcher predicts initial conditions which lead to an uncompleted trajectory, the entire approach bogs down, since the error can no longer be evaluated and the next guess cannot be predicted. Thus, the integrator is required to complete trajectories even for somewhat unreasonable choices of the initial conditions, since the root searcher will usually make a few guesses afield before beginning to converge to the root. On the other hand, the root searcher cannot go too far afield and still maintain good prospects for converging, because trajectories with sufficiently pathological initial conditions will indeed not complete.

There is one other requirement for the root searcher. Since the method must be applied in the real world where computing budgets are finite, the root searcher must be efficient, requiring relatively few trajectories to find the root. For example, if a root searcher converges on the fifth trajecotry, doing an average over N Monte

Carlo points entails running 5N trajectories, 80% of which will be discarded, that is, their results will not be included in the averaging process. Since running trajectories is by far the most time-consuming task in the computation, this amounts to a waste of 80% of the computing time. Similarly, if the root searcher is successful on the tenth guess, only ten percent of the computed trajectories are retained, i.e., used to calculate the desired cross-section. For this reason, the standard multidimensional minimization routines, which typically require fifty or so evaluations of the function to converge to the root, connot be used in the partially-averaged classical-limit method. The root searches tested were required to converge to the root within ten or at most fifteen trajectories, thus giving retention ratios of seven to ten percent. It was deemed that schemes retaining less than five percent of the computed trajectories were too inefficient to be considered viable production methods.

A. H_2-Li^+

Chronologically, the first attempt to apply the partially-averaged classical-limit method was made on the H_2-He system. (Miller and Raczkowski, 1972). This preliminary calculation yielded somewhat unpromising results, for reasons ultimately tracable to the potential surface, and computation on H_2-He was suspended in favor of H_2-Li^+. (A fuller account of this early work will be presented in the section on H_2-He.) In the context of the introduction to this chapter, to describe the calculations on H_2-Li^+

one must define the potential surface, the complex time path chosen in running the trajectories, and the root search used to satisfy the double-ended boundary conditions.

The total potential for the problem can be viewed as consisting of an internal potential for H_2 and an interaction potential for the system at large. The internal potential was taken to be a Morse function,

$$v(r) = D(e^{-2\alpha(r-r_0)} - 2e^{-\alpha(r-r_0)}), \tag{3.3a}$$

with the parameter values

$$D = 0.17443263 \text{ hartree} \tag{3.3b}$$

$$\alpha = 1.04435 \quad a_0^{-1} \tag{3.3c}$$

$$r_0 = 1.40083 \quad a_0 \ . \tag{3.3d}$$

Test calculations were also done with a polynomial fit to the Kolos-Wolniewicz potential (Waech and Bernstein, 1967). The difference in results between the two potentials were negligible. The interaction potential was chosen to be the analytic fit given by Lester (1971) to his <u>ab inito</u> calculated values. This is the same interaction potential used in the coupled-channel calculation on H_2-Li^+ (Schaefer and Lester, 1973). In essence the fit consists of three Legendre terms (corresponding to P_0, P_2 and P_4, since the diatomic is homonuclear); in each term the dependence on the translational coordinate is exponential repulsion with R^{-3} and R^{-4} attraction (leading to an angle-dependent well-depth of a few tenths of an eV),

and the dependence on oscillator separation is linear plus quadratic for the (translational) attraction terms and linear times exponential for the repulsion terms.

Having chosen the potential surface, one then encountered the two-fold problem of running trajectories and performing root searches. The question of choosing the complex time path will be treated first. As was pointed out in the introduction, the only requirement is that the real part of the time difference between the start and end of the trajectory tend to infinity. It is reasonable then, to require that at each step the real part of the time increment be non-negative. There is no restriction, however, on the imaginary part. The integration of the trajectory is carried out in cartesian coordinates using a fifth-order variable-step Adams predictor and Moulton corrector (Miller and George, 1972). At each step the routine evaluates the error (i.e., the difference between the predicted and corrected values) and compares it to some specified tolerance value. If the error is too large the step is repeated with a smaller time increment; if the error is within the tolerance value, the step is accepted and the error is used to determine the magnitude of the next time increment. Thus, one need only specify the phase of each time step to fully determine the time path.

The phase of the time step then, can be varied to assure that the oscillatory motion does not become unbounded. The first attempt to carry this through was based on the premise that, since the

vibrational motion traces an ellipse in the complex plane (with the turning points as foci), the oscillator should be made to pass through, or at least very close to, the turning points on each "oscillation" (Doll and Miller, 1972). The major axis of the ellipse is then only slightly larger than the distance between turning points, and the resulting motion is bounded. The scheme was implemented numerically in the following way. Since the trajectory is being run in Cartesian coordinates, one has at each step the vectors $\vec{R}$, $\vec{r}$, $\vec{P}$, $\vec{p}$ (all with complex components) and their derivates: $\dot{\vec{R}}$, $\dot{\vec{r}}$, $\dot{\vec{P}}$, $\dot{\vec{p}}$. One can then compute p_r, the oscillator's radial momentum at each step by the relation

$$p_r = \vec{p}\cdot\vec{r}(\vec{r}\cdot\vec{r})^{-1/2} \tag{3.4}$$

The time steps are taken to be real with the magnitude determined by the integrator until the oscillator is near a turning point, defined as a value of r for which the radial momentum is zero. The oscillator is considered to be in the vicinity of a turning point when the real part of the radial momentum goes through a sign change. One now wishes to choose the phase of the time increment to bring the oscillator to, or near, the turning point. To do this, one computes the derivative of the radial momentum, given by

$$\dot{p}_r = (\dot{\vec{p}}\cdot\vec{r} + \vec{p}\cdot\dot{\vec{r}})(\vec{r}\cdot\dot{\vec{r}})^{-1/2} - p_r\vec{r}\cdot\dot{\vec{r}}(\vec{r}\cdot\vec{r})^{-1}. \tag{3.5}$$

One then makes the usual linear approximation for the time step:

$$\Delta p_r = \dot{p}_r\cdot\Delta t \tag{3.6}$$

If the radial momentum is to be set to zero, then Δp_r must be proportional to minus p_r; the time step can then be set by

$$|\Delta t| = \min(h, |p_r/\dot{p}_r|) \tag{3.7a}$$

$$\arg(\Delta t) = \arg(-p_r/\dot{p}_r) \tag{3.7b}$$

where h is the magnitude chosen by the integrating routine. One continues to choose the time step according to algorithm (3.7) until the oscillator is within some specified small distance of the turning point. Then one reverts to real time steps fixed by the integrator until the real part of the momentum again changes sign.

This scheme was quite successful in stabilizing complex trajectories, allowing successful completion of 90% of the trajectories attempted. However, because a root searcher will predict perhaps ten or so sets of initial conditions before converging to the root and it will require a successful trajectory for each set of initial conditions, a ten percent rate of failure among trajectories can cause failure of the root search in over half of the Monte Carlo points, caused only by uncompleted trajectories.

Such a difficulty can be overcome in one of two ways. Either the root searcher's predicting algorithm can be modified so that, if its current guess results in an uncompleted trajectory, it chooses initial conditions at random until it completes a trajectory and then uses the results along with those of its previous, say, four guesses to continue the search, or one must improve the method of choosing the complex time path for the trajectories. To anticipate later discussion, the first method proved totally unworkable. The random

guess was usually far from the root; its inclusion in the input to the predicting algorithm further eroded the routine's predictive power, resulting in another pathological guess of initial conditions, which must again be supplanted by random ones, and so on. The effect on convergence to the root was disasterous: the method degenerated into a four-dimensional random walk, which is known the diverge.

It became clear that further refinement in the choice of the complex time path was necessary. Examination of the failing trajectories revealed that the cause of the majority of the failures was a subtle inconsistency in algorithm (3.7). As mentioned earlier, one expects the time increment to always have a positive real part, corresponding to the system's motion forward in time. Equation (3.7b) allows the time increment to have any phase, including those leading to negative real parts. In principle, allowing increments with negative real parts is equivalent to forcing the system to move backwards in time, retracing part of its trajectory in reverse. In practice, the problem can lead to the back-and-forth oscillation of all the trajectory functions which is usually associated with time-reversal, but this only happens if both real and imaginary parts are reversed. If only the real part is reversed, the condition will typically manifest itself by causing the oscillator to circle around a turning point or spiral into it.

A variety of ad hoc elaborations of the basic algorithm were tired to remedy this reversal of the real part of the time. They each engendered more difficulties than they alleviated. The problem was finally solved by focusing on the oscillator separation rather

than the momentum. One can define the oscillator separation r by

$$r = (\vec{r}\cdot\vec{r})^{1/2} \tag{3.8a}$$

Its derivatives are given by

$$\dot{r} = (\vec{r}\cdot\dot{\vec{r}})/r \tag{2.8b}$$

$$\ddot{r} = (\dot{\vec{r}}\cdot\dot{\vec{r}} + \vec{r}\cdot\ddot{\vec{r}})/r - (\dot{r})^2/r. \tag{3.8c}$$

The acceleration vector $\ddot{\vec{r}}$ can be found by differentiating the defining relation for the momentum:

$$\vec{p} = m\dot{\vec{r}} \tag{3.9a}$$

$$\ddot{\vec{r}} = \dot{\vec{p}}/m \tag{3.9b}$$

One then makes a parabolic approximation for the time step:

$$\Delta r = \dot{r}\Delta t + 1/2\ \ddot{r}\ (\Delta t)^2. \tag{3.10a}$$

One would now like to force the oscillator to move toward r_0, its equilibrium position, <u>i.e.</u>,

$$r = -(r-r_0). \tag{3.10b}$$

This defines the time path by the relations

$$|\Delta t| = h \tag{3.11a}$$

$$\mathrm{Arg}(\Delta t) = \mathrm{Arg}\left(\frac{-(\dot{r})^2 \pm ((\dot{r})^2 - 2\ddot{r}(r-r_0))^{1/2}}{\ddot{r}}\right) \tag{3.11b}$$

where the sign before the square root is chosen so that Δt will have a positive real part. Algorithm (3.11) is used to choose the phase of the time increment at every step of the trajectory, until the

asymptotic region is reached. There the oscillator is forced to a turning point in order to facilitate the transformation for Cartesian to action-angle variables. This scheme has proven highly successful in stabilizing the trajectories. The current success rate for complex trajectories is 99+%, the root-search failure rate due to uncompleted trajectories is correspondingly low, less than five percent.

The last aspect of the computational details to be discussed is the root search. In accord with the remarks made previously the root searches considered were required to converge within ten or so iterations. This restriction eliminated the usual multidimensional approach of minimizing the difference between the desired and calculated final conditions by use of a nonlinear least-squares minimizing routine. The root searches which were developed and tested can all be considered to follow the same procedure. One postulates some functional form for the dependence of the final action variables on the initial angles. On the basis of previously run trajectories one solves for the parameters defining the function. One equates the now known function of the initial angles to the desired final value of the action variables and solves for the values of the angles which satisfy this relation. These values are the new predicted root. One then runs a trajectory to test the accuracy of the prediction. If the root is found the process stops, if not, the results of the current trajectory are used along with several previous ones to re-determine the functional parameters.

The simplest example, and in some sense the prototype of the later root searches, occurs in the case of vibrationally inelastic one-dimensional collinear trajectories. The task is to find the value of q_{n_1} such that n_2 is equal to some desired integer, say zero, if one is interested in the de-exitation $n_1 = 1 \rightarrow n_2 = 0$. For simplicity the subscript on q_{n_1} will be suppressed. The root search assumes that n_2 can be expanded as a function of q in a Fourier series truncated after the first-order terms:

$$n_2 = f(q) = A + B \sin q + C \cos q. \tag{3.12}$$

If one has run three trajectories, say with $q = 0, \pi/3, -\pi/3$, resp., and if f_i, s_i, c_i represent respectively n_2, sin q, cos q for the ith trajectory, the parameters A, B, and C of Eq. (3.12) can be found by solution of the equation

$$(f_1, f_2, f_3) = (A, B, C) \begin{pmatrix} 1 & 1 & 1 \\ s_1 & s_2 & s_3 \\ c_1 & c_2 & c_3 \end{pmatrix} \tag{3.13a}$$

The solution is easily obtained by right-multiplying both sides of the equation by the inverse of the 3 x 3 matrix. Once the values A, B and C are known, one solves the relation

$$n_2 = A + B \sin q + C \cos q = 0 \tag{3.13b}$$

to predict the value of q which will satisfy the desired final boundary condition. The usual trigonometric substitution

$$\cos q = (1 - \sin^2 q)^{1/2} \tag{3.14}$$

yields the following as a prediction for the root:

$$q = \arcsin\left(\frac{-AB \pm C(B^2+C^2-A^2)^{1/2}}{B^2+C^2}\right) . \tag{3.15}$$

A trajectory is run with this value of q and if the value of n_2 is less than some specified tolerance parameter, q is considered to be the desired root. If the value of n_2 is too large, the root search continues by substituting the results of the current trajectory and the two previous ones into Eq. (3.12) to redefine the parameters A, B and C and then applying Eq. (3.15) to generate the next approximation to the root.

It will be noted that Eq. (3.15) predicts two roots, depending on which sign is chosen for the second term of the numerator. This is indicative of the general case. Real roots, if they occur, will number 2^n, n being some positive integer, and there will always be complex roots. These can be grouped into pairs, one member of the pair being the complex conjugate of the other. (Miller and George, 1972). As stated previously, complex roots need be considered only if there are no real roots, since the weighting function for complex roots is exponentially damped with respect to that of the real ones. For the same reason, in the absence of real roots only the pair of complex roots with the smallest imaginary parts (corresponding to the weakest damping) need be considered. The two roots are complex conjugates. The argument of the damping

function is the imaginary part of ϕ, ϕ being the integral defined by Eq. (2.59b). One can show that ϕ is an analytic function of the root; thus complex conjugation of the root will complex conjugate ϕ, that is, change the sign of its imaginary past. This means that of the two roots being considered, one leads to exponential damping and the other to exponential enhancement. Clearly, only the root leading to damping has physical significance. However, since the two contributions differ only in the sign of the argument of the exponential, only one of the roots need be found. One can be sure of computing the contribution properly by using minus the absolute value of $\mathrm{Im}(\phi)$ in the argument of exponent, as was done in Eq. (2.60).

In the partially-averaged, three-dimensional case, one sees that the root search problem for real trajectories, as defined by Eq. (2.62), is the same as for the one-dimensional case discussed above. For complex trajectories the situation is more complicated. The root search problem is defined by Eqs. (3.2). The expressions are somewhat cumbersome, and for the purposes of the present discussion it is convenient to write them more compactly. One defines the vector f and q by

$$f = \begin{pmatrix} \mathrm{Re}\ n_2 \\ \mathrm{Im}\ n_2 \\ \mathrm{Im}\ j_2 \\ \mathrm{Im}\ \ell_2 \end{pmatrix} \quad ; \quad q = \begin{pmatrix} \mathrm{Re}\ q_{n_1} \\ \mathrm{Im}\ q_{n_1} \\ \mathrm{Im}\ q_{j_1} \\ \mathrm{Im}\ q_{\ell_1} \end{pmatrix}. \tag{3.16a,b}$$

For simplicity, the usual vector notation has been suppressed. Equation (3.2) requires that the root q_r satisfy

$$f_r = f(q_r) = \begin{pmatrix} n_2 \\ 0 \\ 0 \\ 0 \end{pmatrix}. \tag{3.17}$$

The simplest root searching scheme for this problem results from linearization of f about some value q_0, i.e., the approximation

$$f(q) = f(q_0) + \underline{C}(q-q_0), \tag{3.18}$$

Where $\underline{C}$ is some matrix of constants depending only on the choice of q_0. The scheme can be outlined in the following way.

Step 0: Initialization. Run five trajectories; let f_i and q_i represent the values of the vectors f and q for the ith trajectory.

Step 1: Define the function by linearizing about q_5. Define the matrixes $\underline{F}$ and $\underline{Q}$ by

$$\underline{F} = (f_1-f_5, \ldots, f_4-f_5) \tag{3.19a}$$

$$\underline{Q} = (q_1-q_5, \ldots, q_4-q_5) \tag{3.19b}$$

(since f and q are 4-D column vectors, $\underline{F}$ and $\underline{Q}$ are 4 x 4 matrices.) The coefficient matrix $\underline{C}$ is easily shown to be

$$\underline{C} = \underline{F}\,\underline{Q}^{-1} \tag{3.20}$$

Step 2: Predict root. One wishes to find the value of q_r such that Eq. (3.17) is satisfied. An approximate q_r is given by

$$q_r \approx q_5 + \underline{C}^{-1}(f_r-f_5) \tag{3.21}$$

One runs the trajectory with the approximate q_r. If $|f-f_r|$ is sufficiently small the search stops, if not, the results of the current trajectory and the four previous ones are used as imput to Step 1 to recompute the matrix $\underline{C}$. (Note that in each iteration one linearizes about a different point.)

The root search as outlined was not very successful. The linearizing approximation (3.18) is a very poor one globally and can be expected to have some validity only in the immediate vicinity of q_0. If the q's used to determine the coefficient matrix are too widely separated, the resulting linearization may have no validity. (As an example, consider linearizing a parabola. A carefully chosen line segment may be a reasonable interpolation over a small region and a poor extrapolation outside that region, but a linearization using points on opposite branches will be a poor approximation

everywhere.) The difficulty can be lessened if one started the linear search from a crude approximation to the root, rather then from the real axis. This was done by leaving the last two components of q as zero and varying the real and imaginary parts of q_{n_1} to satisfy

$$\mathrm{Re}\ n_2 = n \tag{3.22a}$$

$$\mathrm{Im}\ n_2 = 0 \tag{3.22b}$$

Once that value of q_{n_1} was found, the linear search was initiated to find the full root. The search in q_{n_1} was done using the 1-D Fourier search procedure described above. The only modification were that f, q, and the expansion coefficients were considered complex, and the functions e^{iq} and e^{-iq} replaced sin q and cos q, since the latter pair tended toward linear dependence for sizeable imaginary parts of q.

The combined procedure (i.e., 1-D Fourier followed by 4-D linear,) was able to find roots at about half the Monte Carlo points, which, it is sad to say, made it the most successful of the root searches discussed here. Initialization of the Fourier search required three real trajectories (equivalent in computational effort to one complex trajectory), covergence to a satisfactory preliminary value of q_{n_1} required three or four complex trajectories, then initialization and convergence of the linear search required eight to ten more complex trajectories. (The initialization of the linear search maximally utilized existing information: by using the last three trajectories run by the Fourier search, the process required only

two additional trajectories, with non-zero values for Im q_{j_1} and q_{ℓ_1} resp., to initialize). Thus the root search required twelve to fifteen trajectories at each Monte Carlo point. The principal cause of failure was the one already discussed. If the predicted root lies far from the point about which f is linearized the guess is likely to be a poor one, because Eq. (3.18) has little validity there. The results of the poor guess are used to recompute $\underline{C}$. The resulting linearization is likely to be poor everywhere, because the input points are widely spaced. The next prediction is likely to be even worse than the previous one. With two bad guesses the $\underline{C}$ matrix is further degraded and the method becomes a four-dimensional random walk. Thus the root search procedure either converged rapidly or diverged rapidly: failure to converge in ten trajectories was a definite indication of serious problems, not merely the result of premature termination. Several modifications of the basic procedure were attempted in the hope of increasing the chances for convergence. The only one which offered any promise was restricting the step size. The root predictor (3.21) may be rewritten as

$$q_r \simeq q_5 + \Delta q, \tag{3.23}$$

where Δq is the second term in the R.H.S. of Eq. (3.21). The idea is to let the predictor give the direction of Δq, but its magnitude is restricted to the region where Eq. (3.18) is valid. Since the region of validity is small, the modified process exhibited a much slower rate of convergence than its predecessor, requiring over

thirty trajectories to converge. Furthermore, it showed only about a ten percent improvement in the success rate. Thus, the modification was not considered useful.

It became clear that significant improvement in the root search procedure would require a new approach. In view of the success of the 1-D Fourier search to locate the approximate root described above, it was felt that extension of the idea to four dimensions was worth investigating. To carry this through, one first expands the variables n, j and ℓ in a Fourier series in q_n, q_j and q_ℓ, retaining only the lowest-order terms. (The usual numerical subscripts have been suppressed in the present discussion. It is clear that one means the <u>final</u> action variables and the <u>initial</u> angles.) Because the diatomic is homonuclear, q_j and q_ℓ have period π, and their lowest order terms in the expansion have argument 2q. Thus the expansion for n is

$$n \approx a_7 + a_1\sin(q_n) + a_2\cos(q_n) + a_3\sin(2q_j) + a_4\cos(2q_j) + a_5\sin(2q_\ell) + a_6\cos(2q_\ell). \qquad (3.24)$$

Similar expansions hold for j and ℓ. The coefficients are all real because real values of the angles lead to real values for the action variables. For complex values of the angles, one applies the standard identites

$$\sin(q) = \sin(\mathrm{Re}\, q)\cosh(\mathrm{Im}\, q) + i\cos(\mathrm{Re}\, q)\sinh(\mathrm{Im}\, q) \qquad (3.25a)$$

$$\cos(q) = \cos(\mathrm{Re}\,q)\cosh(\mathrm{Im}\,q) - i\,\sin(\mathrm{Re}\,q)\sinh(\mathrm{Im}\,q) \quad (3.25b)$$

to separate real and imaginary parts of the expansions. With the definitions

$$q = \mathrm{Re}\,q_n \quad (3.26a)$$

$$x = \sinh(2\mathrm{Im}\,q_j) \quad (3.26b)$$

$$y = \sinh(2\mathrm{Im}\,q_\ell) \quad (3.26c)$$

$$z = \sinh(\mathrm{Im}\,q_n)\ , \quad (3.26d)$$

the conditions for the final action variables become

$$0 = \mathrm{Im}\,n \approx (C_{11}\sin q + C_{12}\cos q)\,z + C_{13}x + C_{14}y \quad (3.27a)$$

$$0 = \mathrm{Im}\,j \approx (C_{21}\sin q + C_{22}\cos q)\,z + C_{23}x + C_{24}y \quad (3.27b)$$

$$0 = \mathrm{Im}\,\ell \approx (C_{31}\sin q + C_{32}\cos q)\,z + C_{33}x + C_{34}y \quad (3.27c)$$

$$\begin{aligned} n_2 = \mathrm{Re}\,n \approx{}& (C_{12}\sin q - C_{11}\cos q)\sqrt{1+z^2} + C_{41} \\ &+ C_{42}(\sqrt{1+x^2}-1) + C_{43}(\sqrt{1+y^2}-1)\ , \end{aligned} \quad (3.27d)$$

where the C's are real coefficients related to the a's of Eq. (3.24) and its analogues for j and ℓ. The search proceeds in the same way as the linear scheme. After running initializing trajectories to determine the coefficients on the first iteration, one substitutes the now known coefficients into Eqs. (3.27), solves them to predict the root, and runs a trajectory to check for convergence. If the root has not yet been found, the new trajectory is used along with

0 0 0 0 4 3 0 3 4 6 6

several of the old ones to recompute the C's and predict a new root, and so on. The equations involved in this method are more tedious than those required in the linearization scheme. Therefore, the present method will be described less explicitly than the previous scheme.

Initialization was accomplished with three real trajectories and two complex ones. The usual real trajectories with $q_n = 0$, $\pi/3$, $-\pi/3$ were run. With these results as input, Eq. (3.15) was used to predict crude values of $Re(q_n)$ and $Im(q_n)$. At this complex value of q_n, two complex trajectories were run with non-zero values of $Im(q_j)$ and $Im(q_\ell)$ resp. Solution for the coefficients was straightforward and required the results of five trajectories. The initializing trajectories were used on the first iteration, and the last five trajectories to be run were used on subsequent iterations. Since the values of Re(n) were known for all five trajectories, evaluation of Eq. (3.27d) for each trajectory gave a system of five linear equations for the unknown coefficients C_{11}, C_{12}, C_{41}, C_{42} and C_{43}. Solution requires inversion of a 5 x 5 matrix. With C_{11} and C_{12} known, the results of the last two trajectories determine C_{13} and C_{14}, requiring 2 x 2 matrix inversion. Solution for the other coefficients proceeded analogously, making use of the analogues of Eq. (3.27d) for Re(j) and Re(ℓ). Solution for the coefficients in the j and ℓ expansions requires inversion of the same two matrixes inverted in the n solution. Since inversion of the 2 x 2 matrix is trivial, the main effort in solving for the coefficients is spent

on a 5 x 5 matrix inversion.

The next step in the procedure, prediction of the root to give the values of the coefficients, requires solution of Eqs. (3.27) for q, x, y and z. The solution is straightforward but algebracially tedious; thus the process will be described rather than given explicitly. One first considers Eqs. (3.27a, b, c) as a set of homogeneous linear equations in x, y and z. If the system is to have a non-trivial solution, the determinant of the "coefficient" matrix must vanish:

$$\begin{vmatrix} C_{11}\sin q + C_{12}\cos q & C_{13} & C_{14} \\ C_{21}\sin q + C_{22}\cos q & C_{23} & C_{24} \\ C_{31}\sin q + C_{32}\cos q & C_{33} & C_{34} \end{vmatrix} = 0 \qquad (3.28)$$

Expansion of the determinant yields a readily found algebraic expression for tan q, which is too tedious to be quoted here. With the value of q fixed, one can solve for x and y in terms of z. Substitution into Eq. (3.27d) yields

$$f(z) = \alpha_0 + \alpha_1 \sqrt{1+z^2} + \alpha_2(\sqrt{1+A^2z^2} - 1) + \alpha_3(\sqrt{1+B^2z^2} - 1) \qquad (3.29)$$

where A, B and the α's are algebraic functions of the C's, sin q, cos q, and n_2, the desired final vibrational action. The value of q is already known, and x and y are known in terms of z, with proportionality constants A and B, resp. Thus solution of Eq. (3.29) for z will completely determine the predicted root. Solution of Eq. (3.29) proceeded in two steps: first a crude guess for the

solution was generated, then the value was refined by either a quadratic or a Newton-secant method. The crude guess was generated by the following procedure. First, all the square roots were expanded for small values of z. The terms in z^2 and z^4 were retained. The resulting equation was solved by quadratic formula for z^2. If the solution were non-negative, it was used as the starting point for the refining search. If no acceptable solution was found for small z, an asymptotic expansion was done for large z. The resulting equations contained a constant term and terms in z and z^{-1}. Multiplication by z gave a quadratic equation whose solution, if it existed, was used as the crude guess. If again there was no acceptable solution, the value of the function was computed at the origin and at a value z_ℓ sufficiently large that the asymptotic expansion was valid. If the function exhibited a sign change, the refining search started with these two points. If there was no sign change, a marching procedure was instituted. The interval between zero and z_ℓ was divided into twenty sub-intervals and function values were checked for a sign change between the end points of each sub-interval. If no sign change was found, one assumed that Eq. (3.29) had no real solution and the entire root search procedure stopped.

Before being applied to the problem of interest, the procedure described above was tested on model problems in which it had to find roots of functions defined by Fourier series with higher-order terms present. The method failed to converge if the higher-order coefficients were more than one-tenth of the lowest order coefficients.

Predictably, the method had little success with the problem of boundary conditions for complex trajectories. A priori, one assumed that the procedure would work well because the expansion (3.24) and its analogues may be valid globally, if the coefficients are well-chosen and if indeed the higher-order Fourier terms are small. Of course, if the expansions are only a moderately good approximation to the true functional dependence of the action vaiables on the angles, part of the difficulty of the root search may lie with the method of determining the expansion coefficients, which uses data on the real part of the an action variable to compute coefficients in the expansion of its imaginary part. If Eq. (3.24) and its analogues were exact, the procedure would be valid; however, if they hold only approximately, the optimum coefficient values in the expansions of the real and imaginary parts may differ. The first modification was to utilize all the information available to compute the coefficients. The problem was then overdetermined, and the coefficients were found by a least squares procedure.

The least-squares solution for the coefficients is somewhat tedious. As an illustration, the coefficients in the n expansion will be found; the solution for the coefficients in the j and ℓ expansions proceeds analogously. Given the results of several trajectories one seeks the coefficients in the expansion equations

$$\mathrm{Re}\ n = f \approx \sum_{i=1}^{5} C_i\ u_i \tag{3.30a}$$

$$\text{Im } n = g \approx C_1 v_1 + C_2 v_2 + D_3 v_3 + D_4 v_4 \tag{3.30b}$$

which will minimize the fitting error, defined by

$$E = \sum_k w_k (f_k - \sum C_i u_{ik})^2 + \sum_k w_k (g_k - \sum C_i v_{ik} - \sum D_i v_{ik})^2 \tag{3.31}$$

The variables f_k, g_k, u_{ik}, v_{ik} represent the values of f, g, u_i, v_i for the kth trajectory under consideration, and w_k represents a weighting factor, if one wishes to do a weighted least-squares solution. The correspondence between Eqs. (3.30) and (3.27a, d), which defines the u's and v's, is readily apparent. To minimize E one sets the partial derivatives of E w.r.t. the coefficients equal to zero, and then solves the resulting equations for the coefficients. By making the definitions

$$F_j = \sum_k w_k f_k u_{jk} \tag{3.32a}$$

$$G_j = \sum_k w_k g_k v_{jk} \tag{3.32b}$$

$$U_{ij} = \sum_k w_k u_{ik} \cdot u_{jk} \tag{3.32c}$$

$$V_{ij} = \sum_k w_k v_{ik} \cdot v_{jk} \ , \tag{3.32d}$$

one can show that the defining equations for the optimal coefficients are for j=1,2

$$F_j + G_j = \sum_{i=1}^{2} C_i (U_{ij} + V_{ij}) + \sum_{i=3}^{5} C_i U_{ij} + \sum_{i=3}^{4} D_i V_{ij} \tag{3.33a}$$

for j=3 thru 5,

$$F_j = \sum_{i=1}^{5} C_i U_{ij} \tag{3.33b}$$

for j=3,4

$$G_j = \sum_{i=1}^{2} C_i V_{ij} + \sum_{i=3}^{4} D_i V_{ij} \ . \tag{3.33c}$$

These may be rewritten more compactly as

$$\vec{H} = \vec{C} \cdot \underline{X} \tag{3.34a}$$

where

$$\vec{H} = (F_1+G_1,\ F_2+G_2,\ F_3,\ F_4,\ F_5,\ G_3,\ G_4), \tag{3.34b}$$

$$\vec{C} = (C_1,\ C_2,\ C_3,\ C_4,\ C_5,\ D_3,\ D_4) \tag{3.34c}$$

and

$$\underline{X} = \begin{pmatrix} U_{11}+V_{11} & U_{12}+V_{12} & U_{13} & U_{14} & U_{15} & V_{13} & V_{14} \\ U_{21}+V_{21} & U_{22}+V_{22} & U_{23} & U_{24} & U_{25} & V_{23} & V_{24} \\ U_{31} & U_{32} & U_{33} & U_{34} & U_{35} & 0 & 0 \\ U_{41} & U_{42} & U_{43} & U_{44} & U_{45} & 0 & 0 \\ U_{51} & U_{52} & U_{53} & U_{54} & U_{55} & 0 & 0 \\ V_{31} & V_{32} & 0 & 0 & 0 & V_{33} & V_{34} \\ V_{41} & V_{42} & 0 & 0 & 0 & V_{43} & V_{44} \end{pmatrix} \tag{3.34d}$$

Solution for the coefficients requires inversion of the 7 x 7 matrix $\underline{X}$. The coefficients in the expansions for j and ℓ were found analogously, requiring only modification in the definition of F and G. Since the basis functions in each expansion are the same, the matrix $\underline{X}$ does not change. Thus one inversion yields all three sets of coefficients. The weighting factors in Eqs. (3.31) and (3.32), if used, were taken to be

$$w_k = (\varepsilon_k)^{-1} \cdot \min (\varepsilon_k) \ , \tag{3.35}$$

where ε_k is the error associated with the kth trajectory, that is, the difference between the desired and calculated final values for the action variables. The largest weighting factor can be taken as unity without loss of generality, since multiplying each factor by a constant, equivalent to rescaling the L.H.S. of Eqs. (3.32), leaves Eqs. (3.33) unchanged. Tests on model problems indicated that the procedure worked best with the weighting factors all set to unity, amounting to a non-weighted scheme, and results of the last five function evaluations included in the sums of Eqs. (3.32). Convergence was slower, since the values of the coefficients did not change as rapidly with new data as in the original version, and the success rate in dealing with higher-order Fourier terms showed only a marginal increase over the original version. The improvement in handling the complex-trajectory final boundary-value problem was also slight.

One more variant of multi-dimensional Fourier searches was attempted. In this one, the coefficients were allowed to become

complex, thereby doubling the number of fitting parameters and, it was hoped, increasing the flexibility of the expansions. The method can be outlined as follows. First one defines f_1, f_2, f_3 to be n, j, ℓ, resp. One may then write expansion (3.24) and its analogues as

$$f_i = \sum a_{ij} u_j \tag{3.36}$$

where the a's are the (now complex) expansion coefficients and u_1 thru u_6 are the various sines and cosines appearing in Eq. (3.24), and u_7 is unity, the function multiplying the coefficient a_7 in Eq. (3.24). Seven real trajectories are used to initialize the scheme. As usual, one defines the matrices $\underline{F}$ and $\underline{U}$ with elements f_{ik} and u_{jk} representing the value of f_i and u_j for the kth trajectory. It is convenient in later iterations to separate real and imaginary parts in solving for the coefficients. (Of course, on the first iteration all the imaginary parts are zero.) One writes, using a super-matrix notation,

$$(\mathrm{Re}\underline{F},\ \mathrm{Im}\underline{F}) = (\mathrm{Re}\underline{A},\ \mathrm{Im}\underline{A}) \cdot \begin{pmatrix} \mathrm{Re}\underline{U} & \mathrm{Im}\underline{U} \\ -\mathrm{Im}\underline{U} & \mathrm{Re}\underline{U} \end{pmatrix} \tag{3.37}$$

Solution requires inverting a 14 x 14 matrix. This method of finding the coefficients has two advantages: first, it uses real arithmetic, and second, it manifestly keeps the coefficients real unless forced to do otherwise. That is, as long as the real part of the action variables depends only on the real part of the expansion

functions and analogously for the imaginary part, the coefficients will remain real.

Predicting the root requires solution of the set of equations

$$\sum a_{1j}\ U_j = 0\ , \tag{3.38a}$$

$$\mathrm{Im}\ (\sum a_{2j}\ U_j) = 0\ , \tag{3.38b}$$

$$\mathrm{Im}\ (\sum a_{3j}\ U_j) = 0\ . \tag{3.38c}$$

To solve the system, one first uses Eq. (3.38a) to find $\sin(q_n)$ and $\cos(q_n)$ in terms of q_j and q_ℓ. Substituting the results into Eqs. (3.38b, c) gives the reduced system

$$\mathrm{Im}\ f_2(\mathrm{Im}\ q_j,\ \mathrm{Im}\ q_\ell) = 0 \tag{3.39a}$$

$$\mathrm{Im}\ f_3(\mathrm{Im}\ q_j,\ \mathrm{Im}\ q_\ell) = 0 \tag{3.39b}$$

The root of Eqs. (3.39) is found by a generalization to two dimensions of the Newton-Raphson scheme. On each iteration one assumes the functions can be approximated as

$$\begin{pmatrix} \mathrm{Im}\ f_2 \\ \mathrm{Im}\ f_3 \end{pmatrix}_{\mathrm{new}} \approx \begin{pmatrix} \mathrm{Im}\ f_2 \\ \mathrm{Im}\ f_3 \end{pmatrix}_{\mathrm{old}} + \frac{\partial(\mathrm{Im}\ f_2,\ \mathrm{Im}\ f_3)}{\partial(\mathrm{Im}\ q_j,\ \mathrm{Im}\ q_\ell)} \cdot \begin{pmatrix} \Delta q_j \\ \Delta q_\ell \end{pmatrix} \tag{3.40a}$$

where the derivative matrix is evaluated at the old value of q_j and q_ℓ. The variables Δq_j, Δq_ℓ are the corrections to the imaginary parts of q_j and q_ℓ. It will be recalled that the real parts of these angles are specified by the Monte Carlo

procedure; the root search can modify only the imaginary parts. At each step, the correction to the root of Eqs. (3.39) is predicted by

$$\begin{pmatrix} \Delta q_j \\ \Delta q_\ell \end{pmatrix} = - \left(\frac{\partial(\mathrm{Im}\ f_2,\ \mathrm{Im}\ f_3)}{\partial(\mathrm{Im}\ q_j,\ \mathrm{Im}\ q_\ell)} \right)^{-1} \cdot \begin{pmatrix} f_2 \\ f_3 \end{pmatrix}_{\mathrm{old}} . \tag{3.40b}$$

The derivative matrix is easily found, since the Cauchy criteria for the differentiability of functions with complex arguments require, <u>inter alia</u>, that

$$\mathrm{Re} \left(\frac{\partial(f_2,\ f_3)}{\partial(q_j,\ q_\ell)} \right) = \frac{\partial(\mathrm{Im}\ f_2,\ \mathrm{Im}\ f_3)}{\partial(\mathrm{Im}\ q_j,\ \mathrm{Im}\ q_\ell)} . \tag{3.41}$$

The derivatives of L.H.S. of Eq. (3.41) can be found by differentiating Eqs. (3.36) for f_2 and f_3, keeping in mind that $\sin q_n$ and $\cos q_n$ are now defined as functions of q_j and q_ℓ by use of Eq. (3.38a). Once Eqs. (3.39) are solved, the usual process of running a trajectory, checking the results, and recomputing the coefficient matrix to make the next prediction of the root is followed. On subsequent iterations, if the imaginary part of any of the angles (usually q_n) becomes substantial, it may be necessary to use e^{iq} and e^{-iq} in place of $\sin(q)$ and $\cos(q)$ in the coefficient determination, since the second pair of functions tends toward linear dependence. This poses problems only in the solution for the coefficients; the solution of Eqs. (3.38) is unaffected.

Application of the various four-dimensional Fourier searches to the problem of interest resulted in rather disappointing success rates.

The procedures were able to find roots in less than twenty percent of the Monte Carlo points sampled. This is appreciably worse than the more simple-minded approach using the linearizing approximation. The unexpected failure of the Fourier methods prompted an attempt to gauge the importance of higher-order terms in the Fourier expansions of n, j and ℓ. For a randomly chosen impact parameter and total angular momentum several hundred real trajectories were run: a coarse grid was set up in q_n and q_j, and at each grid point trajectories corresponding to fifty equally spaced q_ℓ values between 0 and π were run. The idea was to Fourier analyse the results at each grid point to obtain the coefficients of the q_ℓ terms. (Naturally, the "coefficients" would be function of q_n and q_j.) Two more sequential Fourier analyses, first for different values of q_j at fixed q_n and then for different values of q_n, would determine the coefficients in Eq. (3.24) and higher-order corrections. However, only the analysis for q_ℓ was completed. It showed that for different (q_n, q_j) grid points there were from six to thirty q_ℓ - terms with comparable coefficients. Usually n had the most rapidly converging series, and ℓ was somewhat slower to converge than j. The most apparent conclusion, however, was that Fourier expansions retaining only lowest-order terms could not possibly be expected to give a reasonable representation of the actual functional dependence involved. Thus a search based on such expansions was most probably doomed to failure, at least at the one Monte Carlo point discussed here. In practice, the usual manifestation of failure at a Monte Carlo point was a breakdown

in the solution of the equations predicting the root. Since these equations were to be solved by an iterative numerical procedure, it was not clear whether the expansion broke down, i.e., the equations had no solution because of pathological values for the coefficients, or whether the numerical procedure was merely unable to find a solution which did in fact exist. Thus besides the fundamental question of the validity of the expansion, there is the additional practical complication that the equations predicting the root are not amenable to easy analytic solution.

A curious point to ponder is the observation that the linear search exhibited a higher success rate than the first-order Fourier searches. One would expect a Fourier expansion of n, j and ℓ w.r.t. the angles to converge faster than a Taylor series, primarily because the Fourier basis functions have the correct periodicity built into them. Yet the search based on truncating the more slowly converging series does better than one based on the more rapidly convergent series. The resolution of this seeming paradox may lie in the differing natures of the two expansions. The salient properties will emerge from a consideration of the one-dimensional case.

The one-dimensional analogue of the linearization scheme is the Newton-secant method. If the two points determining the secant line coalesce, one recovers the Newton-Raphson method, which amounts to truncation of the Taylor series after the linear term. If one has

$$f(x+\Delta x) = f(x) + \sum_{n=1}^{\infty} \frac{1}{n!} f^{(n)}(x)\cdot(\Delta x)^n \quad , \tag{3.42}$$

one knows that for small enough Δx, the linear term will dominate the sum. Thus the linear method gives a good approximation locally and a poor one globally, reflecting the nature of the Taylor series as an approximation about a point. On the other hand, the Fourier series is an approximation on an interval. Its primary concern is a global one--periodicity. One has then

$$f(x) = a_0 + \sum a_n \cos(nx) + \sum b_n \sin(nx) \tag{3.43a}$$

$$f(x+\Delta x) \approx f(x) + \Delta x(\sum n \cdot b_n \cdot \cos(nx) - \sum n \cdot a_n \cdot \sin(nx)) \tag{3.43b}$$

It is assumed that $f(x)$ has period 2π, and only the lowest-order term in Δx was retained in Eq. (3.43b). Inspection of Eqs. (3.43) reveals two disconcerting observations. First, neglect of higher-order Fourier terms in Eq. (3.43a) implies neglect in Eq. (3.43b) of terms first-order in Δx. Second, neglect of small terms in the first equation may lead to neglect of much larger terms in the second equation. Because the coefficients in the sums of Eq. (3.43b) contain an added factor of n, it is clear that a truncation which gives a reasonable value of $f(x)$ may give very unreasonable values for its derivatives, and thus may give a good representation globally and a poor one locally. One concludes that if the coefficients of higher-order Taylor terms are appreciable, the linear procedure gives an approximation to the function which is guaranteed to be good on some small interval about x and poor beyond that interval. In the first-order Fourier procedure, if higher-order

coefficients are important, one has an approximation which is exact at the three points used to determine the first-order coefficients and poor everywhere else, although it will predict global properties better than local ones. Numerical root-searching procedures are dependent on local properties, since one is usually given f(x) and seeks a Δx such that $f(x + \Delta x)$ will be zero. This is fundamentally a local problem. Thus it is reasonable, in retrospect, to expect the linear search to do better, unless the function is represented extremely well by a first-order Fourier series. The latter seems to be the case for $n_2(q_n)$, which would explain the success of the complex 1-D Fourier search in q_n.

Doubtlessly a contributing factor to the success of the combined 1-D Fourier, 4-D linear search was the location of the root. In all cases where a root was found, the imaginary parts of q_j and q_ℓ were small, less than one-tenth. Thus once the approximate value of q_n was found by the complex 1-D Fourier procedure, the linear search was initiated very close to the root, thereby rendering its chances of convergence good. It was hoped that this location of the root could be exploited by a different type of root-search. This final root-searching effort involved alternating application of two root-searches. First a complex 1-D Fourier search was done in q_n to set n to its desired value. Then with q_n fixed, a 2-D linear search varied Im q_j and Im q_ℓ to set Im j and Im ℓ to zero, changing the value of n in the process. Now the values of Im q_j and Im q_ℓ were fixed and q_n was again varied to return n to its desired value, and so on. This procedure was more time-consuming

than the 1-D Fourier, 4-D linear; and it showed a lower success rate. Since the 50% success rate of the best root-search was considered unacceptably low, the 4-D root-search problem was circumvented by neglecting the last two terms in ϕ, i.e.,

$$(q_j \cdot j) + (q_\ell \cdot \dot{\ell})$$

(see Eq. (2.59b). It was felt that this approximation to ϕ, in effect a neglect of the rotational and orbital contributions to the forbiddenness of the transition, was justified by the small values of the imaginary parts of q_j and q_ℓ. The resultant simplification of the root-search required only that the (complex) equation

$$n_2(q_n) = 0 \tag{3.44}$$

be satisfied. The problem was easily handled by the complex 1-D Fourier search in q_n. The procedure showed a 95% success rate when applied to this problem.

The results of this study have been published previously (Raczkowski and Miller, 1974) and will only be briefly summarized here. Figure 2 shows the cross sections for vibrational de-activation of H_2 by Li^+--i.e., $\sigma_{n_2 j_2 \leftarrow n_1 j_1}(E_1)$ for $(n_1, j_1) = (1,0)$ and $n_2 = 0$--for total energy E = 1.2 eV. The values labeled SC are the present classical-limit results, and the error bars indicate the satistical error in the Monte Carlo average; 1000 Monte Carlo points were used.

The points designated QMI in Fig. 2 are the results of Schaefer and Lester's quantum mechanical calculation with a coupled channel

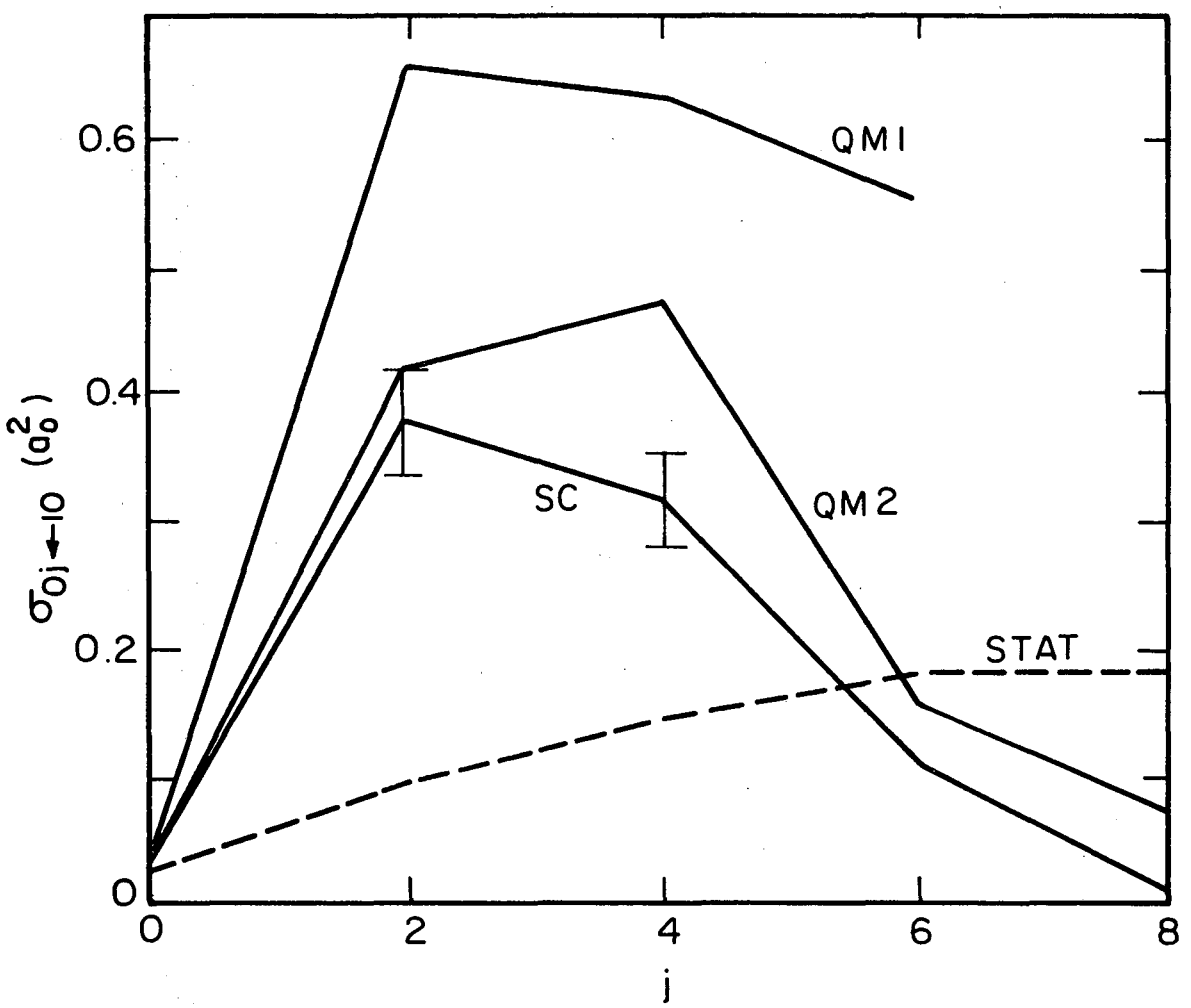

XBL 748-6935A

Fig. 2. Final j-state distribution for scattering from the (0,1) state of H_2-Li^+ at E = 1.2 eV (total) QM1, QM2 -- coupled-channel results
SC -- Classical-limit calculation
STAT -- Statistical distribution.

expansion including the states

$$n = 0;\ j = 0, 2, 4, 6, 8, 10 \qquad (3.45)$$
$$n = 1;\ j = 0, 2, 4$$
$$n = 2'\ j = 0, 2$$

The values labeled QM II are their results obtained by adding one additional rotational state to each vibrational manifold: $j = 12$ for $n = 0$, $j = 6$ for $n = 1$, and $j = 4$ for $n = 2$.

The large change in the quantum results with this increase in basis set seems to indicate that the coupled channel expansion is still some ways from convergence, a rather disconcerting observation since the basis set already produces up to 75 coupled channels. (It should be noted that Schaefer and Lester were primarily interested in pure rotational transitions, $n_1 = n_2$, and their results do indicate the expansion to be converged for these processes.) Another possibility is that the difference between the QM I and QM II results is due to numerical error, since the algorithm used for solving the coupled equations does not seem well-suited for treating processes with small transition probabilities.

The cross section summed over final rotational states, $\sigma_{n_2 \leftarrow n_1 j_1}$ for $(n_1, j_1) = (1,0)$ and $n_2 = 0$, is 1.87 a_o^2, 1.15 a_o^2, and 0.83 a_o^2, respectively, for the QM I, QM II, and classical-limit calculations. Within the uncertainty of the quantum mechanical results, therefore, the classical-limit cross sections are in excellent agreement with the quantum values, both in magnitude and in the

distribution of rotational states (Fig. 2) populated in the vibrational de-activation.

Finally, it is interesting to ask what the rotational state distribution in Fig. 2 signifies about the dynamics of the inelastic process. First, one sees that a substantial amount of the energy released by the vibrational de-activation goes into rotational excitation. The amount of rotational excitation is considerably less than that of a "resonant" process (no change in translational energy), however which would require a final rotational state $j_2 = 8$. It is also interesting to compare to a <u>statistical</u> distribution of final rotational states; this corresponds to

$$\sigma_{0j_2 \leftarrow 10}(E_1) \approx (2j_2 + 1)\ [E - \varepsilon(0,j_2)]\ , \qquad (3.46)$$

where E is the total energy and $\varepsilon(0,j_2)$ the vibrational-rotational energy of H_2 for n= 0 and $j = j_2$. This distribution, normalized to the classical-limit cross section, is the dashed line in Fig. 1. The amount of rotational excitation is thus also much less than that based simply on available phase space.

B. H_2-He

As stated earlier, the H_2He system was the subject of the first three-dimensional application of the partially-averaged classical-limit theory (Miller and Raczkowski, 1972). The results obtained were not very encouraging, since they showed that a large fraction of the trajectories did not complete. The problem was ultimately traced to the fitting form of the interaction potential. The potential surface used in this study was based on the ab initio calculations of Gordon and Secrest (1970). Of the several calculations presented in their paper, only the one labelled AASCF(5,2,2) provides values of the potential for non-equilibrium separations of the diatomic. The authors provide an analytic fit for this potential, given as

$$V(r,R,\gamma) = Ce^{(\Delta r\cdot\alpha_1-\alpha_o)\cdot R}(A(\gamma)-B(\gamma)\cdot\Delta r), \qquad (3.45)$$

where the coordinates are as illustrated by Fig. 1 (Δr is the deviation from the equilibrium oscillator separation), and all the parameters are intrinsically positive. If one considers R and γ fixed and looks merely at the potential's dependence on r, the first factor is an exponential in Δr with positive coefficient, and the second factor is linear with negative slope. Clearly then, for large r the potential becomes infinitely attractive with increasing r, that is, the potential becomes negative and exponentially large. In all fairness to the authors one must point out that the breakdown of the fitting form occurs far from the region where the ab inito values are known, whereas the authors stipulate that their form is intended only for interpolation between the ab inito points and caution against its use for extrapolating

the potential. One should also note that the total potential consists of the interaction potential and the potential for isolated H_2. In the case of real trajectories, for example, the latter term would confine the system to a small region about the equilibrium position. However, complex trajectories can tunnel into the H_2 potential until they reach the region where the spurious values of the interaction potential dominate.

Because of these difficulties with the potential surface the calculations on the H_2-He system were suspended in favor of H_2-Li^+. After the completion of the H_2-Li^+ study outlined earlier, attention turned once again to H_2-He. Since successful continuation of the project would at least have required refitting the Gordon-Secrest data to a less problematic functional form, it was decided to start afresh with the ab inito values calculated by Tsapline and Kutzelnigg. These points were fitted to an analytic form; however, preliminary calculations indicated that the potential at atom-diatom separations smaller than those used by Tsapline and Kutzelnigg were also important. Thus the potential was extended to shorter R-distances (see Fig. 1) using the joint MOLECULE-ALCHEMY program package, which incorporates the MOLECULE integral program and the ALCHEMY SCF program. MOLECULE was written by Dr. J. Almlöf of the University of Uppsala, Sweden. The ALCHEMY SCF program was written by Drs. P. S. Bagus and B. Liu of the IBM San Jose Research Laboratory. The interfacing of these programs was performed by Drs. U. Wahlgren (presently at the University of Uppsala) and P. S. Bagus at IBM. For a description of MOLECULE

see J. Almlöf, "Proceedings of the Second Seminar on Computational Problems in Quantum Chemistry," p. 14, Strassburg, 1972 (Max-Planck Institute, Munich 1973). For a description of the ALCHEMY-SCF program, see: P. S. Bagus, "Documentation for ALCHEMY - Energy Expressions for Open Shell Systems" IBM Research Report RJ 1077 (1972). The ALCHEMY quantum chemistry programs were written primarily by P. S. Bagus, B. Liu, A. D. McLean and M. Yoshimine of the Theoretical Chemistry Group at IBM Research in San Jose, California. Preliminary descriptions of the program are given in: (a) A. D. McLean, "Potential Energy Surfaces from ab initio Computation: Current and Projected Capabilities of the ALCHEMY Computer Program," Proceedings of the Conference on Potential Energy Surfaces in Chemistry held at the University of California, San Cruz, August 1970; and (b) P. S. Bagus, "ALCHEMY Studies of Small Molecules," Selected Topics in Molecular Physics, Verlag Chemie (1972).

The calculation consisted of a Roothaan approach to the SCF, followed by a CI with all single and double excitations. Each configuration is a pure spin eigenfunction with S = 0. The number of configurations used depends on the symmetry being considered (Roos, 1972). In all, three angles (and related symmetries) were considered (see Fig. 1): $\gamma = 0$, or collinear approach ($C_{\infty v}$ symmetry), $\gamma = \pi/4$ (C_s), and $\gamma = \pi/2$, or perpendicular approach (C_{2v}). The basis set used by Tsapline and Kutzelnigg consisted of gaussian lobes. For He, the 7s basis set of Huzinaga was contracted (3,1,1,1,1) following Dunning. It was augmented by three sets of p-groups with orbital exponents

η = 1.6, 0.6, 0.22, and a set of d-groups with η = 0.8. Each H was described by the 6s Huzinaga basis set in the (3,1,1,1) contraction of Dunning, augmented by three sets of p-groups with η = 1.57, .43, .15 and a d-set with η = .25. This large basis set was necessary for describing the long-range Van der Waals interaction of the system, arising from the correlation term. At the shorter distances probed in the present potential-surface calculations, the interaction is dominated by the repulsive SCF term; correlation provides only a small correction. Thus in the interest of reducing the computational burden, the basis set used here consisted of the same s-functions as above augmented by two sets of p-groups on each center, with orbital exponents η = 1.1, 0.41 for He and η = 1.0, 0.29 for each H.

Table 1 shows a comparison of results for C_{2v} symmetry at R = 4.0 au., r = 1.406 au. The SCF terms for the basis sets are essentially identical, and the smaller basis set gives almost 80% of the CI correction. The discrepancy is due almost exclusively to neglect of the d-functions: a 2pld augmentation on each center gave virtually the same results as the large basis set. Similarly, retaining the three sets of p-groups on each center gave essentially the same result as the 2p augmentation. The last point to be made about the suitability of the basis set is that even at R = 4, a 20% error in the correlation term represents an error of three percent in the total interaction. As one goes to smaller values of R, two trends should further reduce the relative error. First, the SCF term should increasingly dominate over the CI correction, and secondly the relative error in the CI caused by neglect of the d-functions should decrease, because the

0 0 0 0 4 3 0 3 4 7 6

Table I. Basis set comparison*, C_{2v} symmetry, r = 1.406 au.

Basis Set	H[6s3p1d/4s3p1d] He[7s3p1d/5s3p1d]	H[6s2p/4s2p] He[7s2p/5s2p]
E(SCF), R = 4 au	-3.9907871 (H)	-3.9905592 (H)
E(CI), R = 4 au	- .0764175	- .0726905
E(SCF), R = 20 au	-3.9948078	-3.9945912
E(CI) , R = 20 au	- .0755000	- .0719772
ΔE(SCF	+ .0040207	+ .0040230
ΔE(CI)	- .0009175	- .0007133
ΔE(TOT)	+ .0031032	+ .0033187

*See text for contractions and orbital exponents.

very diffuse d-orbitals should become less important in describing the system at close distances. In the region probed, one would expect relative error to be a few parts per thousand, certainly less than one percent.

For each of the three symmetries discussed above the interaction potential was calculated on a grid of points with R = 1.8, 2.2, 2.6 au. and r = 0.9, 1.406, 2.2 au. (The asymptotes for each r-value were calculated in C_{2v} symmetry with R = 20 au.) The results for the C_{2v} and C_s symmetries at each value of R were interpolated quadratically to give the values at r = 1.0 and 1.8 au. The results for r = 2.2 in $C_{\infty v}$ symmetry were suspect because the CI correction was positive, i.e., the correlation in the close-in system was less than in the asymptote. It was felt that this could signal a curve-crossing or some other complication. The collinear calculations were repeated at r = 1.8 with R = 1.8 2.2, 2.6, 3.0 and 3.5 au. The correlation correction was once again positive at R = 1.8. The results were plotted on semi-log paper to reveal a linear relationship for all the points except the first, with R = 1.8, which lay above the line. In other word, the potential was increasing exponentially with decreasing R, as one would expect for an SCF-dominated interaction, until R = 2.2,and then rose more sharply at distances smaller than this. To ease the task of fitting the points, the exponential was extrapolated to R = 1.8, and this value was used in place of the questionable <u>ab initio</u> one. The collinear values at r = 1.0 were obtained by quadratic interpolation of the values at r = 0.9, 1.406, and 1.8 au.

A Legendre analysis was performed on the potential values as a function of angle. The symmetry of the homonuclear diatomic allows only even terms in the Legendre series. At the R-distances used in the present extension, as well as the select points at which Tsapline and Kutzelnigg give results for $\gamma = \pi/4$, the coefficients of the first three Legendre terms, viz., P_0, P_2, P_4, were calculated. At the other Tsapline-Kutzelnigg points, only the coefficients of P_0 and P_2 could be found. The results showed that the P_4 coefficient was negligible for $R > 4$ au. The potential was then fit to the following analytical form.

$$V_I(r,R,\gamma) = V_0(r,R)\cdot P_0(\cos\gamma) + V_2(r,R)\cdot P_2(\cos\gamma) + V_4(r,R)\cdot P_4(\cos\gamma) \tag{3.46}$$

where the coefficients are given by the following relations (all distances are in au., all energies in Hartrees.)

$$V_0(r,R) = A_0(r)\ e^{-2.16789\cdot R} + B_0(r)\ R^{11} e^{-4.216\cdot R} + C_0(r)\cdot R^{-6} \tag{3.47a}$$

$$A_0(r) = 18.532\ (1 + .2451\cdot\Delta r - .1646\ \cdot(\Delta r)^2) \tag{3.47b}$$

$$B_0(r) = 8.146\ (1 + 1.7711\cdot\Delta r + .3886\ \cdot(\Delta r)^2) \tag{3.47c}$$

$$C_0(r) = -5.032\ (1 + .5813\cdot\Delta r - .2347\ \cdot(\Delta r)^2) \tag{3.47d}$$

$$V_2(r,R) = A_2(r)\cdot(1+.311\cdot R\cdot\Delta r)\ e^{-2\cdot R} + C_2(r)\cdot\left(\frac{1-e^{-1.667\cdot R}}{R}\right)^6 \qquad (3.48a)$$

$$A_2(r) = 2.811\ (1 + .7613\cdot\Delta r + .2197\cdot(\Delta r)^2) \qquad (3.48b)$$

$$C_2(r) = -1.067\ (1 + 1.5764\cdot\Delta r + 1.2274\cdot(\Delta r)^2) \qquad (3.48c)$$

$$V_4(r,R) = (A_4(r) + R\cdot B_4(r))\cdot e^{-3.6\cdot R} \qquad (3.49a)$$

$$A_4(r) = 13.4238(1 - 2.4036\cdot\Delta r - 2.0953\cdot(\Delta r)^2) \qquad (3.49b)$$

$$B_4(r) = -1.0024(1 - 29.3771\cdot\Delta r - 27.2996\cdot(\Delta r)^2) \qquad (3.49c)$$

A comparison of ab initio and fitted values is given in Table II; the units are milli-Hartrees (1mH ≈ 300°K). The quality of the fit can be summarized by stating that large relative errors correspond to small absolute errors, and large absolute errors correspond to small relative ones. In view of the restrictions on the fitting form, this is the best that one can reasonably expect. The chief restriction, of course, is that the form must be analytic (in the complex variable sense), so that the potential can be continued into the complex plane. This eliminates the possibility of using different forms in different regions, and thus the single functional form chosen must adequately represent the ab initio values over five orders of magnitude. Judging the adequacy of the fit is problematic since numerical measures of the error, such as least-squares, are not as meaningful as one might expect. For example, in V_0 and V_2 the well-depth is four orders of magnitude smaller than the highest computed point on the repulsive wall. A naive least-squares determination of the coefficients in an "exp-six" form will give a fit which is correct to 0.1% for the highest

Table IIa. Comparison For V_0.

r = 1.0 au

R (au)	Potential (mH)	Fit	Abs. Error	Rel. Error
1.8	221.11538	220.50339	-0.61199	-0.00277
2.2	105.33280	106.69225	1.35945	0.01291
2.6	49.10775	47.67970	-1.42806	-0.02908
4.0	2.34623	2.44200	0.09577	0.04082
6.0	-0.04740	-0.03138	0.01602	-0.33800
8.0	-0.01473	-0.01339	0.00134	-0.09096
10.0	-0.00380	-0.00364	0.00016	-0.04122

r = 1.406 au

R (au	Potential (mH)	Fit	Abs. Error	Rel. Error
1.8	229.60883	229.00071	-0.60813	-0.00265
2.2	115.17960	117.33850	2.15890	0.01874
2.6	56.59436	54.97151	-1.62285	-0.02868
3.0	25.75935	25.49497	-0.26439	-0.01026
4.0	3.35439	3.56826	0.21387	0.06376
5.0	0.26267	0.31978	0.05715	0.21761

0 0 0 0 4 3 0 3 4 7 8

Table IIa. Comparison For V_0. (Cont'd)

r = 1.406 au

R (au)	Potential (mH)	Fit	Abs. Error	Rel. Error
6.0	-0.04707	-0.03574	0.01132	-0.24059
6.5	-0.04787	-0.04371	0.00416	-0.08696
7.0	-0.03940	-0.04556	0.00384	-0.09751
8.0	-0.02020	-0.01849	0.00171	-0.08447
9.0	-0.00993	-0.00940	0.00054	-0.05388
10.0	-0.00523	-0.00502	0.00021	-0.03985

r = 1.8 au

R (au)	Potential (mH)	Fit	Abs. Error	Rel. Error
1.8	229.54969	229.0983	-0.45286	-0.00197
2.2	121.35257	123.34083	1.98826	0.01638
2.6	62.45119	60.46051	-1.99068	-0.03188
4.0	4.55460	4.78582	0.23122	0.05077
6.0	-0.03627	-0.03042	0.00585	-0.16126
8.0	-0.02553	-0.02203	0.00350	-0.13709
10.0	-0.00677	-0.00599	0.00077	-0.11441

Table IIb. Comparison For V_2.

r = 1.0 au

R (au)	Potential (mH)	Fit	Abs. Error	Rel. Error
1.8	31.50332	30.16833	-1.33498	-0.04238
2.2	12.58261	13.59269	1.01008	0.08028
2.6	5.83526	5.77960	-0.05567	-0.00954
4.0	0.26087	0.19400	-0.06687	-0.25633
6.0	-0.00880	-0.00981	-0.00101	0.11498
8.0	-0.00247	-0.00229	0.00018	-0.07133
10.0	-0.00060	-0.00060	-0.00000	0.00180

r = 1.406 au

R (au)	Potential (mH)	Fit	Abs. Error	Rel. Error
1.8	59.49735	53.71098	-5.78637	-0.09725
2.2	24.91813	26.45402	1.53589	0.06164
2.6	12.26209	12.31603	0.05395	0.00440
3.0	5.22535	5.56225	0.33690	-0.06447
4.0	0.73315	0.68447	-0.04868	-0.06640
5.0	0.05935	0.05943	0.00008	0.00131

0 0 0 0 4 3 0 3 4 7 9

Table IIb. Comparison For V_2. (Cont'd)

r = 1.406 au

R (au)	Potential (mH)	Fit	Abs. Error	Rel. Error
6.0	-0.01513	-0.00559	0.00954	-0.63048
6.5	-0.01295	-0.00779	0.00516	-0.39838
7.0	-0.01080	-0.00673	0.00407	-0.37672
8.0	-0.00500	-0.00375	0.00125	-0.24922
9.0	-0.00247	-0.00196	0.00050	-0.20351
10.0	-0.00107	-0.00106	0.00001	-0.00543

r = 1.8 au

R (au)	Potential (mH)	Fit	Abs. Error	Rel. Error
1.8	86.01750	83.22312	-2.79438	-0.03249
2.2	41.83965	43.85438	2.01473	0.04815
2.6	21.00903	21.49706	0.48803	0.02323
4.0	1.60580	1.40625	-0.19955	-0.12427
6.0	-0.01573	-0.00144	0.01429	-0.90853
8.0	-0.00887	-0.00654	0.00233	-0.26265
10.0	-0.00193	-0.00192	0.00002	-0.00889

Table IIc. Comparison For V_4.

R (au)	Potential (mH)	Fit	Abs. Error	Rel. Error
		r = 1.0 au		
1.8	5.37260	10.24889	4.87629	0.90762
2.2	0.67170	1.20033	0.52863	0.78699
2.6	0.21872	-0.00654	-0.22525	-0.02989
		r = 1.406 au		
R (au)	Potential (mH)	Fit	Abs. Error	Rel. Error
1.8	17.74197	17.82208	0.08012	0.00452
2.2	3.59722	4.07684	0.47962	0.13333
2.6	1.05296	0.93139	-0.12157	-0.11545
3.0	0.29979	0.21249	-0.08730	-0.83578
4.0	0.03195	0.00525	-0.02671	-0.83578
5.0	-0.00229	0.00013	0.00241	-1.05604
		R = 1.8 au		
R (au)	Potential (mH)	Fit	Abs. Error	Rel. Error
1.8	30.76614	35.38704	4.62090	0.15019
2.2	10.21711	10.54249	0.32538	0.03185
2.6	2.80045	3.00918	0.20873	0.07453

0 0 0 0 4 3 0 3 4 8 0

two points on the wall and completely obliterates the well. Modification of the least-squares to minimize the relative error also gives poor results, since a 20% error is insignificant if the ab initio value is one degree Kelvin, but very significant if the value is one eV. Thus one must settle for the sort of trade-off described above: small relative error for for small values. Unfortunately, in this approach one loses any clear-cut quantitative criterion for deciding when the fitting parameters have been optimized. One must ultimately make a subjective judgement about when the fit is "good enough".

With the potential defined by Eqs. (3.46) thru (3.49) scattering calculations using both the coupled-channel and the classical-limit techniques were performed at four total energies: 0.9, 1.1, 1.3 and 1.5 eV. The classical-limit calculations were a straightforward application of the methods developed for H_2-Li^+. The partial-averaging and the approximation of neglecting the rotational and orbital contributions to the damping function, both discussed extensively in the previous section, were used to reduce the problems incurred in the root-search. The searching procedure converged for over 90% of the Monte Carlo points with the higher energies showing higher convergence rates than the lower energies. The coupled channel calculations were done using the Lester version of the Gordon program. The nature of the method has been discussed in the previous chapter, and the reader is referred to the articles by Gordon (1970, 1971) and Lester (1973) for further details. All tolerance values in the program were set to 10^{-4}, and the basis set used consisted of the following states:

$$n = 0,\ j = 0,\ 2,\ 4,\ 6,\ 8$$
$$n = 1,\ j = 0,\ 2,\ 4,\ 6 \qquad (3.50)$$
$$n = 2,\ j = 0,\ 2,\ 4$$

The wavefunctions of these states, required to compute the coupling matrix (see Eq. (2.33b), were found by numerical solution of Eq. (2.12c) using the Numerov method with v(r) taken to be the Kolos-Wolniewicz potential.

The calculations yielded a plethora of results. The cross-sections are the first level at which a meaningful comparison can be made between the coupled-channel and classical-limit results. Figure 3 shows the coupled-channel result for $\sigma_{1,0\to0}$ as a function of total energy. The cross-sections for the other initial j-states behave very similarly. They are all approximately equal at .9 eV; the cross-sections for j_1 = 4 and 6 rise somewhat more rapidly, becoming about twice and four times as large, resp., as $\sigma_{1,0\to0}$ at 1.5 e V. It would appear that values of the cross-sections at 1.5 eV are too large. This could be due to neglect of the state (1,8). Pure rotational transitions from the lower j_1 states to (1,8) would, of course, decrease the cross sections for the V-R transitions to the ground state. For reasons stated below, one would expect such large Δj transitions to (1,8) to become more important at higher energies. Figure 4 shows the same quantity, $\sigma_{1,0\to0}$, calculated by the classical-limit method. Qualitatively the behaviour is similar, however the classical-limit results are two to three orders of magnitude larger than the coupled channel results. This is a disasterous showing, especially in view of the quantitative

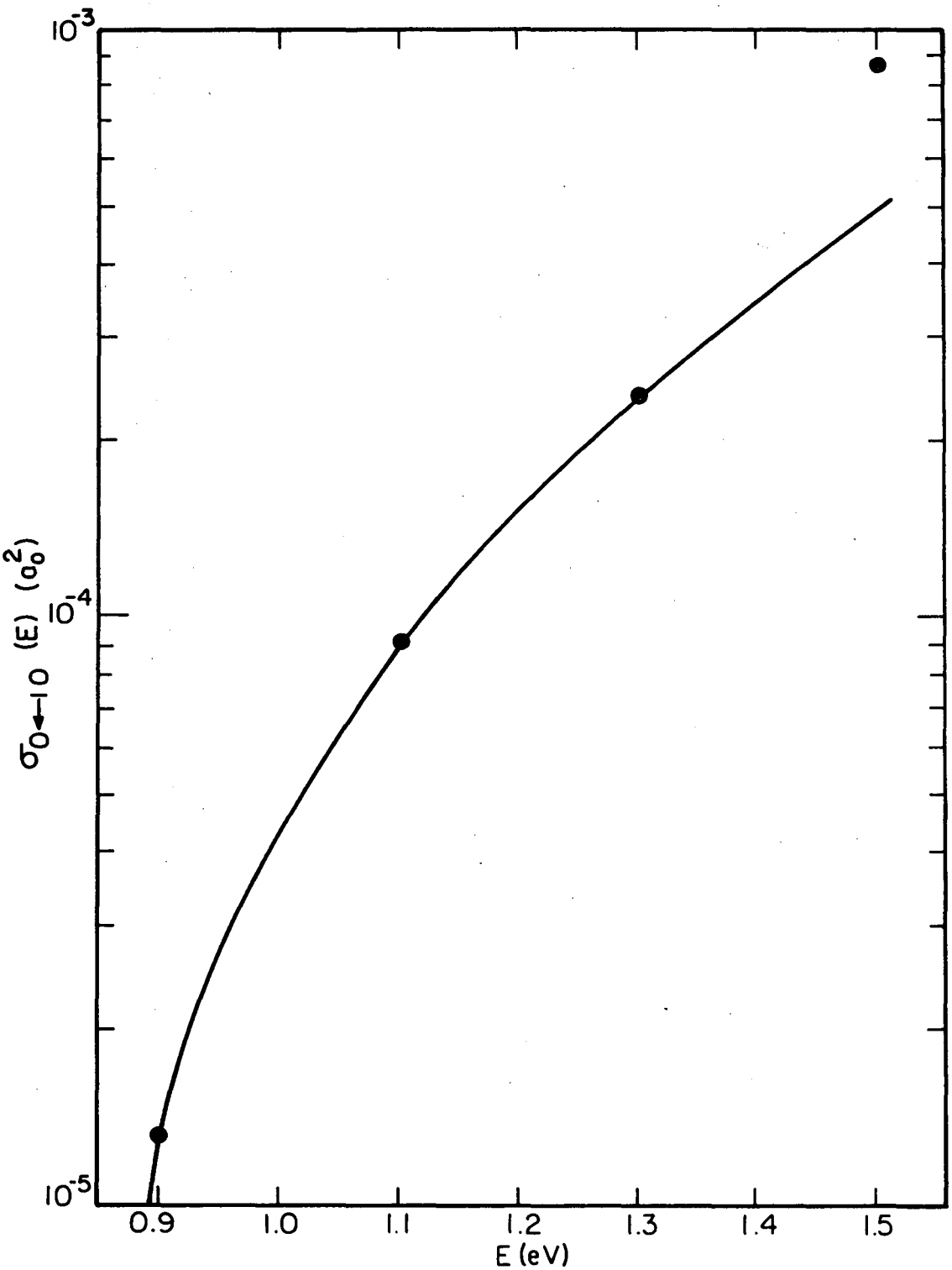

XBL 759-7222

Fig. 3. Cross-section for scattering from state (1,0) to ground vibrational manifold of H_2-He as function of total energy. Coupled-channel results.

0 0 0 0 4 3 0 3 4 8 2

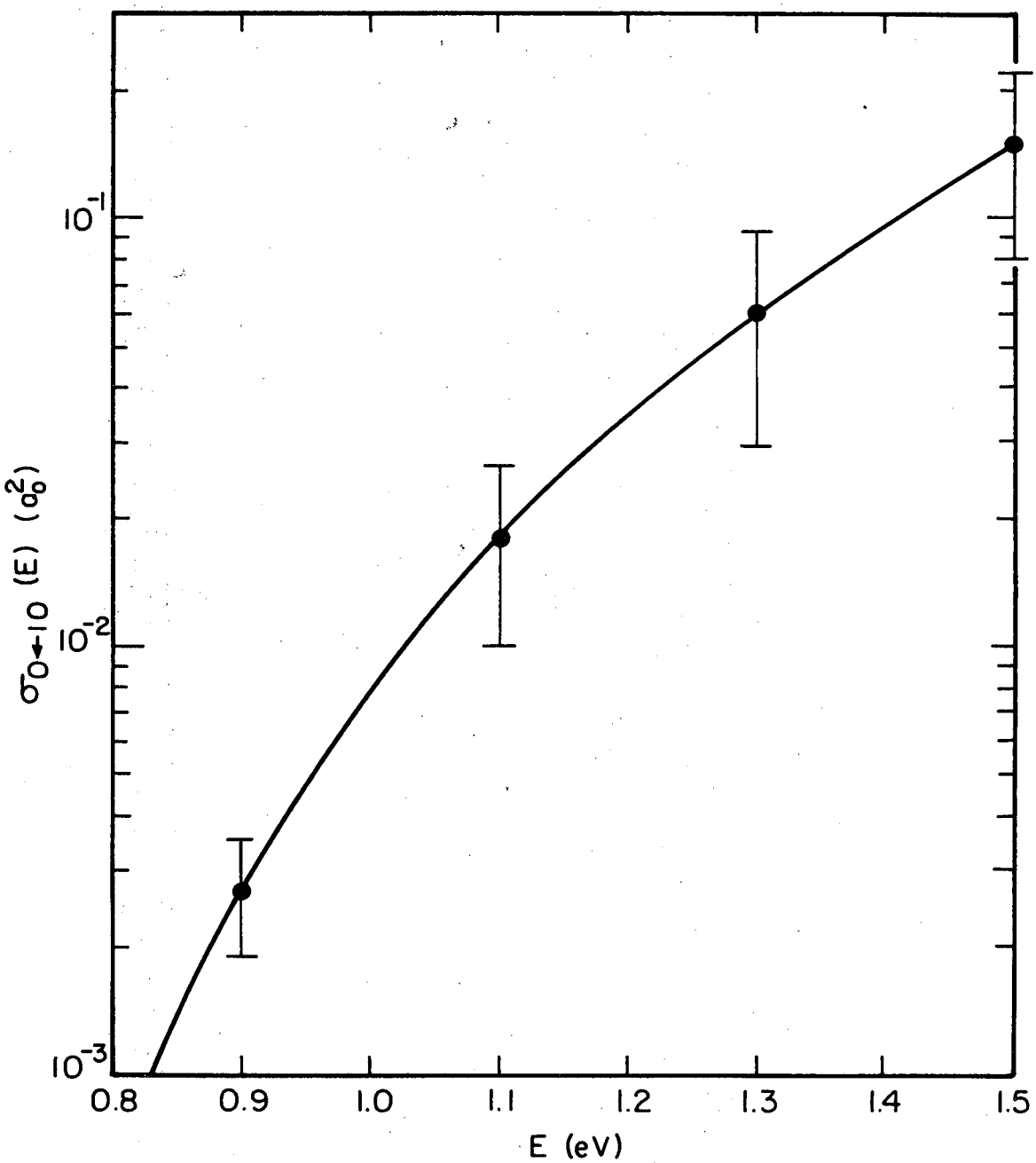

XBL759-7223

Fig. 4. Cross-section for scattering from state (1,0) to ground vibrational manifold of H_2-He as function of total energy. Classical-limit results.

agreement in the H_2-Li^+ study.

It is also illuminating to examine the distribution of final j-states. Figure 5 shows this distribution for scattering arising from the (1,0) state, calculated by the coupled-channel method. Again the other initial j-states follow a well-defined pattern. At .9 eV the scattering from each state peaks at $j_2 = j_1 + 2$; at higher energies the same relation hold for all states except $j_1 = 0$, which peaks at $j_2 = j_1 + 4$. Figure 2 shows that H_2-Li^+ follows a similar distribution. The qualitative features of the final rotational distribution can be rationalized by observing that the system has weak coupling and widely-spaced energy levels. In the limit of no coupling both the internal energy and rotational angular momentum would be conserved. With weak coupling, the system would like to undergo transitions which almost conserve these two quantities. Of course, that is impossible. Small Δj's require large energy changes, on the order of .5 eV if $j_1 = 0$. Similarly, small E's require j's on the order of six or eight. At .9 eV, $\Delta j = 2$ is the most probable transition, with $|\Delta E| = .48, .42, .35, .30$ eV for $j_1 = 0, 2, 4, 6$ resp. at higher energies, $\Delta j = 4$ is more probable for $j_1 = 0$, with $|\Delta E| = .38$ eV. For the other initial j-states, the $\Delta j = 4$ transition also rises more rapidly than $\Delta j = 2$ with increasing total energy, but $\Delta j = 2$ still remains the most probable transition. This trend can be understood by recalling that rotational excitation takes place by transfer of angular momentum from the orbital to the rotational mode. Loss of angular momentum is more likely if the initial orbital angular momentum is large, i.e., $\Delta \ell = -4$ is more likely if

0 0 0 0 4 3 0 3 4 8 3

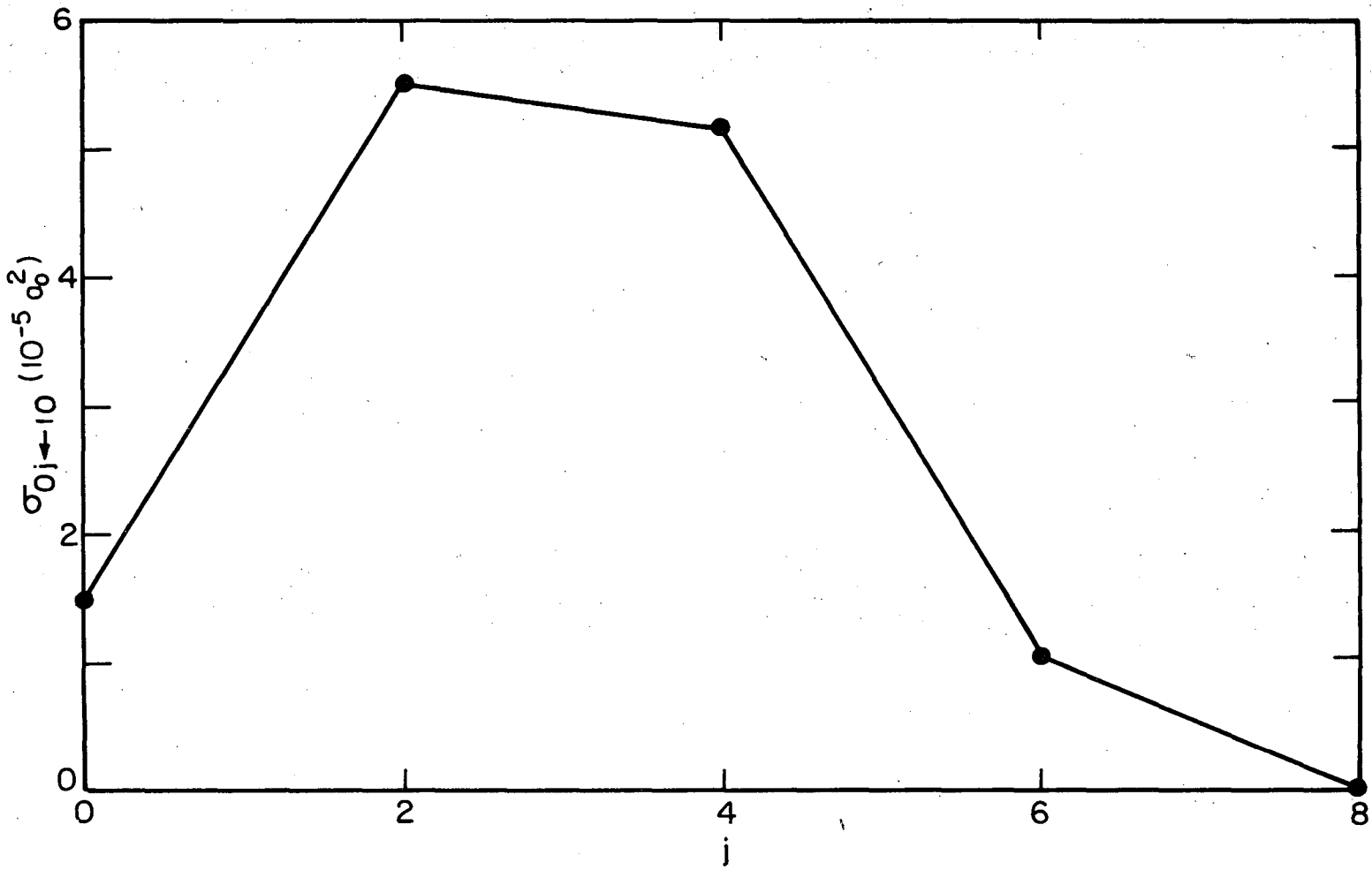

XBL759-7224

Fig. 5. Final j-state distribution for scattering from the (1,0) state of H_2-He at E = .9 eV (total). Coupled-channel result.

$\ell_1 = 30$ than if $\ell_1 = 6$. However, if the interaction potential has a finite range, say b_{max}, the largest orbital angular momentum of any consequence is $\ell_{max} = k\, b_{max}$. For ℓ-values larger than ℓ_{max} the corresponding impact parameter is so large that the system never enters the interaction region and all asymptotic quantities are conserved. The wavenumber k depends on the energy, of course, with the consequence that for fixed b_{max}, ℓ_{max} increases in energy. Thus one would expect $\Delta j = 4$ transitions to increase more rapidly with energy than $\Delta j = 2$ transitions. In the case of $j_1 = 0$, the transitions are roughly comparable at .9 eV, so at higher energies $\Delta j = 4$ becomes dominant. For the other j-states, $\Delta j = 4$ is one or two orders of magnitude smaller than $\Delta j = 2$, so although it rises more rapidly, it does not dominate over $\Delta j = 2$. Of course, the importance of $\Delta j = 4$ transitions at higher energies may invalidate the results for (1,6) cross-sections at 1.5 eV, since the state (0,10) was not in the basis set. Figure 6 shows the final rotational distribution from state (1,0), computed by the classical-limit method. The distribution clearly overestimates the relative probability of the $j = 4$ transition. This seems to be true for other j_1-states and energies as well. It would appear that the very poor showing of the classical-limit results for this system is due to the approximation neglecting the rotational contribution to the damping function. The H_2-He systems exhibits far less angular anisotropy than H_2-Li^+, and apparently the rotational contribution to the "forbiddenness" cannot be neglected, as it was in the H_2-Li^+ calculations. Thus it follows that a successful application of the classical-limit method to H_2-He can only be done

0 0 0 4 3 0 3 4 8 4

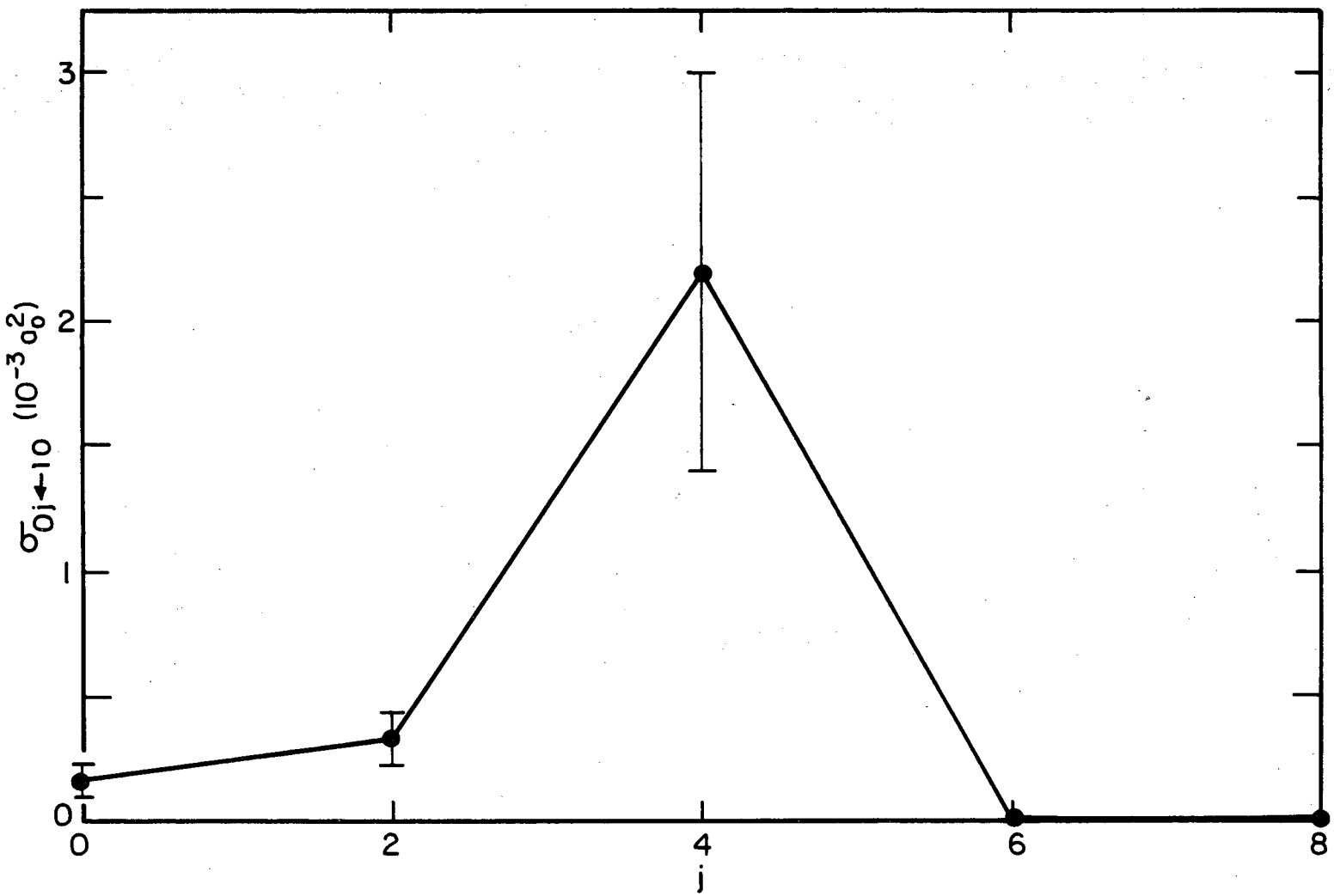

XBL759-7225

Fig. 6. Final j-state distribution for scattering from the (1,0) state of H_2-He at E = .9 eV (total). Classical-limit result.

using the full boundary conditions of Eqs. (3.2) and necessitating the use of a four-dimensional root-search procedure.

The final step in the H_2-He calculations was the use of the cross-section data to find the rate constants and relaxation times. Rate constants connecting specific quantum levels were found by fitting the corresponding quantum cross-sections to a power law and carrying out the integration of Eqs. (2.68). More specifically, to find the rate of transition from state i to f the cross-section was fit to the form

$$\sigma_{f\leftarrow i} \approx A(E_{tr})^p, \tag{3.50}$$

where E_{tr} is the translational energy in state i and the values of A and p were found by taking the logarithm of both sides of the equation and passing a least-squares line through the known points. Substitution of Eq. (3.50) into Eqs. (2.68) and use of Eq. (2.67) gives the following final expression for the rate constant;

$$k_{f\leftarrow i} \approx \left(\frac{8}{\pi\mu}\right)^{1/2} \cdot A \cdot (k_B T)^{(p+\frac{1}{2})} \cdot \Gamma(p+2) \tag{3.51}$$

Of course, only the downward rate constants (i.e., i>f) need be computed this way: the reverse rates are given by the detailed balance relationship (see Eq. (2.76)). Once all the off-diagonal elements of the rate matrix were found the diagonal elements were computed by use of Eq. (2.74).

With the rate matrix known the relaxation rate was computed in two ways. The first approach can be termed a pseudo two-state method, since it makes use of the well-known result that the relaxation rate is given by

$$k_r = k_{0\leftarrow 1}\cdot(1+e^{-\beta\cdot\Delta E}) \tag{3.52}$$

for a system with two levels, labelled zero and one in this case. The variable ΔE is just the energy spacing of the two levels. In applying this approach to H_2-He one approximates the system by two states, corresponding to n=0 and n=1. The relaxation rate is then given by Eq. (3.52) with the parameters defined by

$$k_{0\leftarrow 1} = \frac{\sum_{j_1}\left(\sum_{j_2} k_{0j_2\leftarrow 1j_1}\right)\cdot\left(2j_1+1\right)\cdot e^{-\beta(E_{1j_1}-E_{00})}}{\sum_{j_1}(2j_1+1)\cdot e^{-\beta(E_{1j_1}-E_{00})}}, \tag{3.53a}$$

$$\Delta E = (E_{10}-E_{00}). \tag{3.53b}$$

The second method used was the diagonalization scheme outlined in Section (II.C). The states included in the rate matrix were

$$n = 0,\ j = 0,\ 2,\ 4,\ 6,\ 8$$
$$n = 1,\ j = 0,\ 2,\ 4,\ 6$$

the results of the two methods agreed to better than one-half of a percent for temperatures below 2,000°K.

Relaxation rates were also computed on the basis of the classical-limit scattering results. However, because of the uncertainties in the final j-state distribution of these results the procedure involving

specific quantum levels had to be modified. The cross-sections fit to the power law of Eq. (3.50) were first summed over the final rotational state, i.e., they were of the form:

$$\sigma_{0\leftarrow 1j_1} = \sum_{j_2} \sigma_{0j_2\leftarrow 1j_1} \tag{3.54}$$

Evaluation of Eq. (3.51) then gave an approximate value for $k_{0\leftarrow 1j_1}$. Substitution of this value into Eq. (3.53a) gave the classical-limit relaxation rate, since $k_{0\leftarrow 1j_1}$ can equivalently be defined by

$$k_{0\leftarrow 1j_1} = \sum_{j_2} k_{0j_2\leftarrow 1j_1} \tag{3.55}$$

The diagonalization scheme could not be applied to the classical-limit results for two reasons. The first is the final j-state distribution mentioned earlier. The second is that the scheme requires the rates for purely rotational transitions within the n=0 and n=1 manifolds. The corresponding cross-sections had not been computed in the classical-limit calculations (only vibrationally inelastic transitions were considered), and these rates were not available. However, because of the agreement between pseudo two-state and diagonalization results for the coupled-channel data, it can be presumed that the pseudo two-state results are an accurate representation of the relaxation rate for the classical-limit data.

Figure 7 shows a comparison of the classical-limit, coupled channel, and experimental results for the relaxation rate in the

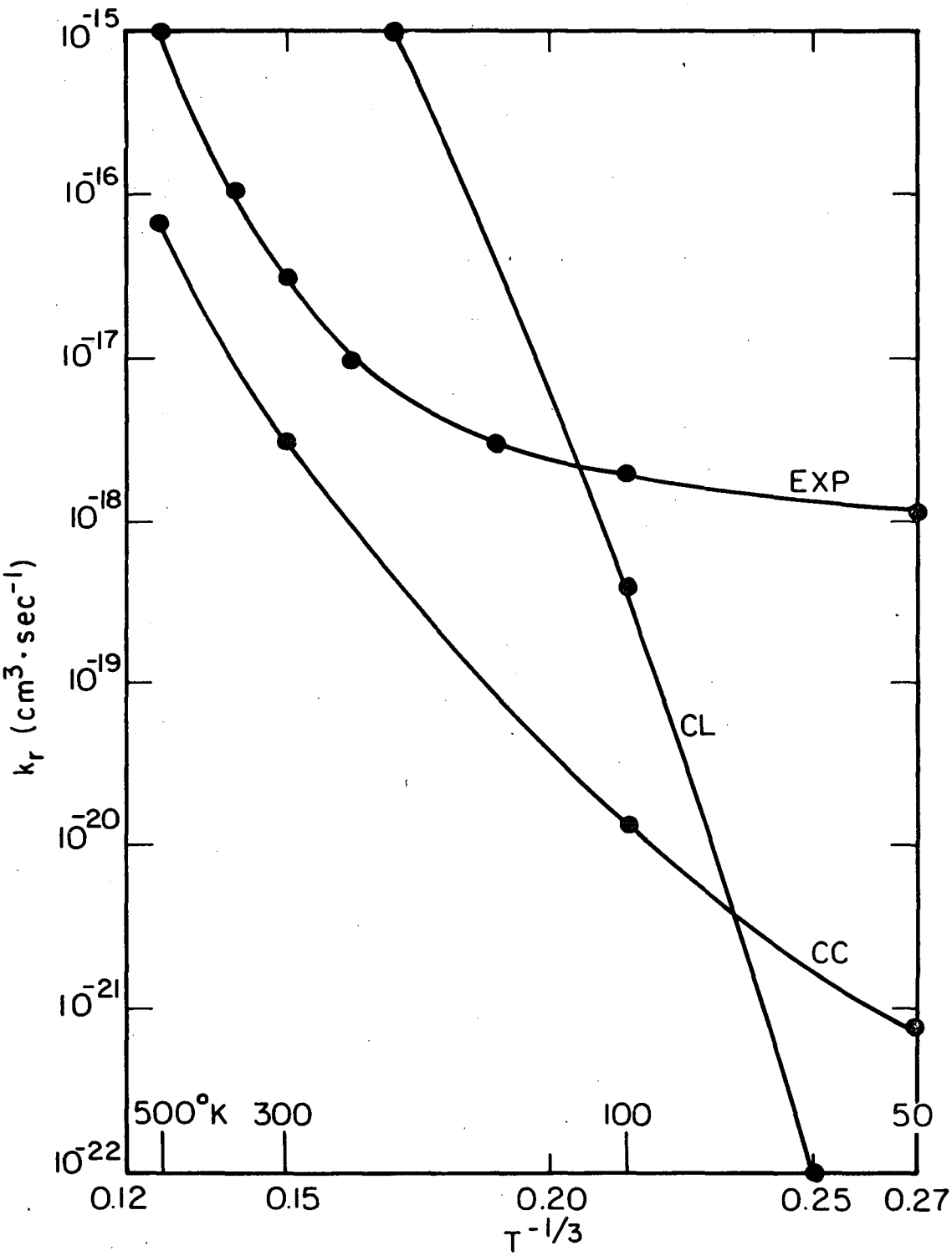

XBL 759-7226

Fig. 7. Relaxation rate for H_2-He system as function of temperature.
CC -- Coupled-channel
CL -- Classical-limit
EXP -- Experiment

temperature range of 50 to 500°K. Clearly the classical-limit results are in very poor agreement with experiment. They predict the wrong curvature and are several orders of magnitude in error over most of the range. The coupled-channel results show much better agreement. The curvature is qualitatively correct but much weaker than that shown by the experimental points. Extension of the curves to higher temperatures (not shown) indicates essentially quantitative agreement in the range of 1500 - 3000°K between the coupled-channel results and the shock-tube data of Dove, Jones and Teitelbaum, as quoted by Audibert, et al. (see Ref. 2 of Audibert, Joffrin and Ducuing). The classical-limit results in this range fall about two orders of magnitude above the experiment.

In order to draw any conclusions from these comparisons one must recall that the underlying cross-sections were computed in the range of .9-1.5 eV total energy, or .3-1.0 eV relative translational energy, since the internal energies of the states dominating the relaxation; namely (1,0), (1,2), (1,4), are about .5-.6 eV. The translational energies correspond to temperatures of 3,000 to 10,000°K. Thus the shock-tube experiments probe the relaxation rate at temperatures comparable or slightly below the energy range of the cross-section calculations. Not suprisingly then, the high-temperature relaxation rates reflect the discrepancy between the coupled-channel and classical-limit cross-sections, with the coupled-channel results being essentially exact.

The low temperature (T<500°K) relaxation results depend sensitively on the behavior of the cross-section immediately above threshold. This behaviour is poorly represented by a power-law extrapolation from higher energies. Below room temperature the relaxation rate is dominated by $k_{0\leftarrow 10}$ (see Eq. (3.53a)), and test calculations indicate that the extrapolation used here would result in a serious underestimate of the underlying corss-section, $\sigma_{0\leftarrow 1,0}$, for E_{tr} < .042 eV (≈460°K). In this energy range vibrational deactivation competes only with elastic scattering: pure rotational transitions to higher states of the n=1 manifold are energetically forbidden. Of course, in the range where the cross-sections were computed purely rotational transitions are allowed; their effect is to reduce the probability of vibrational deactivation. (That is, if the states n=1, j=2, 4, 6 were dropped from the coupled-channel calculation, the effect would be to increase $\sigma_{0\leftarrow 1,0}$.) Extrapolation of the cross-section curve to low energies underestimates the cross-sections around threshold by improperly including the effects of purely rotational transitions, which in fact cannot take place at those energies. It is felt that this is the cause of the discrepancy in degree of curvature between the curvature between the coupled-channel results and the experimental work of Audibert, et. al. Unfortunately, removing this discrepancy would call for very difficult calculations just above threshold to determine the correct cross-section behaviour there. Test calculations show that the S-matrix elements of interest are very small, less than 10^{-8}. Computing

0 0 0 0 4 3 0 3 4 8 8

them reliably would require exacting tolerances. Further, because of the low transitions probabilities involved, it may prove necessary to use the de Vogelaere algorithm in place of the Gordon method used in the present study.

IV. CONCLUSIONS

As stated in the introduction, the purpose of this project was to develop a method of using complex trajectories to extend the applicability of quasi-classical calculations to classically forbidden problems and to test the validity of the proposed method by comparison with essentially exact quantum calculations. Thus there are three basic questions which must be answered by this concluding summary: how well does the proposed method compare with exact calculations, how can the comparison be improved, and what difficulties can be expected in generalization to systems larger than atom-diatom.

The first two questions have, in essence, been answered in the body of this dissertation; however, a recapitulation is in order. Agreement for the H_2-Li^+ system was quantitative, both in the size of the cross-sections and in the distribution of final rotational states. In comparison, agreement for the H_2-He case was very poor. The classical-limit cross-sections were one to two orders of magnitude too large, they rose too sharply, and the distribution of final rotational states peaked at the state immediately above the correct maximum.

The cause of these difficulties is also clear. The angular anisotropy of the H_2-He interaction potential is much smaller than that of H_2-Li^+. Consequently the neglect of the rotational and orbital contributions to the damping integral of Eq. (2.59b) introduced a much more serious error into the results for H_2-He. As expected, an underestimate of the damping function yields an overestimate

of the cross-sections, in this case amounting to at least a factor of ten. Similarly, the final rotational distribution was analyzed as a trade-off between energy and angular-momentum conservation. Since the approximation described above overestimates the ease of rotational-orbital coupling, one would expect the classical-limit distribution to show more internal-energy conservation and thus be shifted to higher final j-values.

It will be recalled that the approximation of neglecting part of the damping integral was introduced to reduce the root-search problem to manageable dimensionality. The original four-dimensional problem proved not to be amenable to easy solution at each point of the Monte Carlo average. The results of the H_2-He study force one to conclude that if the proposed classical-limit method is to be made completely reliable in all cases, the full damping integral must be used and the 4-D root-search must be performed at each Monte Carlo point. This means that if this line of research is to be continued, the first order of business must be the development of a reliable and efficient multidimensional root-searching procedure.

Of course, even in its present state the proposed method is of potential utility. The H_2-Li^+ results show that the method works well if the angular anisotropy of the potential is large, and it is in precisely such cases that coupled-channel calculations become tedious, since many partial waves must be included in the sum for the cross-sections. The proposed classical-limit method can be used to complement exact quantum procedures. In systems with weak rotational coupling, coupled-channel calculations are easily done; the

classical-limit method proposed here can be applied conveniently and reliably to systems with strong rotational coupling.

Lastly, there is the question of extension to larger systems. The first problem is obtaining reliable potential surfaces describing the interaction of such systems. However, since this problem applies to all exact methods, it is not germane to the discussion. As regards extension of the classical-limit formulation to larger systems, the complication of the rotational motion should be tractable without major difficulties. Problems arise, however, from the presence of several vibrational modes. Apart from increasing the dimensionality of the root-search (with "partial-averaging" over rotation, the rotational modes will each contribute one dimension to the root-search; the vibrational modes will each contribute two dimensions), the presence of more than one vibrational mode will necessitate a reexamination of the algorithm use to stabilize complex trajectories.

It will be recalled that the current version of the algorithm varies one independent variable (the argument of the time path) to control the value of one dependent variable (the oscillator separation). In the case of larger systems several dependent variables (corresponding to separations in the several vibrational modes) will have to be bounded. One could, of course, try bounding some suitably weighted sum of such separations; this would at least restore the parity of one independent variable and one dependent variable. Nonetheless, the matter would require careful scrutiny. Thus, extension to larger systems would require a reliable multidimensional

0 0 0 0 4 3 0 3 4 9 0

root-search procedure and a modification of the stabilizing algorthm for complex trajectories.

ACKNOWLEDGMENT

First of all the author wishes to thank Professor William H. Miller for his encouragement and sage counsel throughout the course of this project. Thanks are also due to Dr. William A. Lester, Jr. of the IBM Corporation, whose expertise and computer programs were an invaluable help in the coupled-channel calculations on H_2-He. Secondly, the author wishes to thank former post-docs of the Miller group: Drs. Tom George, Jim Doll, Chris Sloane, and Richard Preston, as well as former colleagues Drs. Barbara Garrison and Stuart Augustin and Mr. Steven Hornstein, all of who have contributed to the author's intellectual growth during the formative years of his graduate career. Discussions with Dr. Garrison were also instrumental in facilitating the potential-surface calculations on H_2-He.

On a more mundane level the author wishes to express his gratitude to the National Science Foundation and to the Inorganic Materials Research Division of the Lawrence Berkeley Laboratory, formerly under the AEC, currently under the U. S. Energy Research and Development Administration, for funding this project. Thanks are also due to the IBM Corporation, which provided computer time for the potential-surface and coupled-channel calculations on H_2-He. Finally the author thanks Ms. Lorine Hesleph and the other members of the Technical Typing Division of IMRD for their efforts in typing this thesis.

0 0 0 0 4 3 0 3 4 9 1

REFERENCES

1. M. Alexander, Chemical Physics, 8, 86 (1975).
2. M. M. Audibert, C. Joffrin and Ducuing, Journal of Chemical Physics, 61, 4357 (1974).
3. J. Doll and W. H. Miller, J. Chem. Phys., 57, 5019 (1972).
4. T. H. Dunning Jr, J. Chem. Phys., 53, 2830 (1970) and 55, 716 (1971).
5. H. Goldstein, Classical Mechanics, Addison-Wesley (1950)
6. M. D. Gordon and D. Secrest, J. Chem. Phys., 52, 120 (1970) and Erratum: 53, 4408 (1970).
7. R. Gordon, J. Chem. Phys., 51, 14 (1969).
8. R. Gordon, Quantum Scattering Using Piecewise Analytic Solutions" in Methods of Computational Physics, Vol. 10, Academic Press (1971).
9. S. Huzinaga, J. Chem. Phys., 42, 1293 (1965).
10. W. Kolos and L. Wolniewicz, J. Chem. Phys., 43, 2439 (1965).
11. W. A. Lester, Jr, J. Chem. Phys., 54, 3171 (1971).
12. W. A. Lester, Jr. and J. Schaefer, J. Chem. Phys., 59, 3676 (1973).
13. W. A. Lester, Jr., The N Coupled-Channel Problem in Modern Theoretical Chemistry, Vol. 3, W. H. Miller, Ed., Plenum Press, to be published (1975).
14. P. McGuire and J. P. Toennies, J. Chem. Phys., 62, 4623 (1975).
15. W. H. Miller, J. Chem. Phys., 53, 1949 (1970).
16. W. H. Miller, J. Chem. Phys., 54, 5386 (1971).
17. W. H. Miller, Classical-Limit Quantum Mechanics and the Theory of Molecular Collisions in Advances in Chemical Physics, Vol. 25 (1974a).

18. W. H. Miller, The Classical S-matrix in Molecular Collisions in Molecular Beams, K. P. Lawley, Ed., Wiley (1974b)

19. W. H. Miller and T. George, J. Chem. Phys., 56, 5668 (1972).

20. W. H. Miller and A. W. Raczkowski, Faraday Discussions of the Chemical Society, 55, 45 (1972).

21. I. Oppenhein, K. E. Shuler and G. H. Weis , Stochastic Theory of Multistate Relaxation Processes in Advances in Molecular Relaxation Processes, Vol. 1 (1967).

22. H. Rabitz and G. Zarur, J. Chem. Phys., 62, 1425 (1975).

23. A. W. Rackowski and W. H. Miller, J. Chem. Phys. 61, 5413 (1974)

24. B. Roos, Chemical Physics Letters, 15, 153 (1972).

25. M. E. Rose, Elementary Theory of Angular Momentum, (Wiley, 1957).

26. J. Schaefer and W. A. Lester Jr., Chem. Phys. Lett., 20, 575 (1973)

27. J. R. Taylor, Scattering Theory (Wiley 1972).

28. B. Tsapline and W. Kutzelnigg, Chem. Phys. Lett., 23, 173 (1973).

29. T. G. Walch and R. B. Bernstein, J. Chem. Phys., 46, 4905 (1967)

30. R. E. Weston Jr. and H. A. Schwarz, Chemical Kinetics (Prentic-Hall 1972).

0 0 0 4 3 0 0 4 9 2

LEGAL NOTICE

This report was prepared as an account of work sponsored by the United States Government. Neither the United States nor the United States Energy Research and Development Administration, nor any of their employees, nor any of their contractors, subcontractors, or their employees, makes any warranty, express or implied, or assumes any legal liability or responsibility for the accuracy, completeness or usefulness of any information, apparatus, product or process disclosed, or represents that its use would not infringe privately owned rights.

TECHNICAL INFORMATION DIVISION
LAWRENCE BERKELEY LABORATORY
UNIVERSITY OF CALIFORNIA
BERKELEY, CALIFORNIA 94720